Faculty of Engineering of University of Porto

Development of a Polymeric Matrix based on Hyaluronic Acid and Dextrin Hydrogels for the Expansion of Undifferentiated Mesenchymal Stem Cells

Joana Martins

Master's dissertation in the context of
Integrated Master in Bioengineering
Major in Biomedical Engineering

Supervisor: Prof. Dr. José Domingos Santos
Co-supervisor: Prof. Dr. Francisco Miguel Gama

June 2014

Resumo

A engenharia de tecidos é uma área emergente que permite o tratamento de várias doenças. Células estaminais mesenquimatosas podem ser usadas nestes tratamentos uma vez que têm a capacidade de se diferenciarem em diferentes tipos de células, incluindo osteoblastos, adipócitos e condrócitos. Contudo, pode ser necessária a sua expansão *in vitro,* previamente à sua utilização em aplicações clínicas, de modo a obter quantidades suficientes. Durante esse período, é necessário que as células estaminais mesenquimatosas se mantenham num estado indiferenciado. Podem para esse efeito ser usados hidrogéis como *scaffolds* devido à sua biocompatibilidade e ao seu alto conteúdo em água que promove a viabilidade celular. Pretende-se neste trabalho avaliar o potencial dos hidrogéis de ácido hialurónico e dextrino na proliferação das células estaminais mesenquimatosas, uma vez que, devido às suas propriedades químicas e mecânicas, estes hidrogéis imitam a matriz extracelular. Assim, estes hidrogéis foram avaliados de modo a determinar a duração do estado indiferenciado das células estaminais mesenquimatosas nestes biomateriais.

Os hidrogéis de dextrino e de ácido hialurónico foram produzidos com diferentes tipos de ácido hialurónico e com diferentes rácios, tendo sido feita uma caraterização com base no grau de oxidação, tempo de gelificação e taxa de degradação. Foram realizados testes preliminares de viabilidade celular através do teste da resazurina e de atividade metabólica através do teste de MTT utilizando células MG-63. Por fim, os hidrogéis foram implantados subcutaneamente em ratos, tendo sido feita uma análise histológica de biocompatibilidade através da Norma ISO 10993. Os resultados mostraram que todos os hidrogéis tiveram um tempo de gelificação curto e que hidrogéis mistos com grandes percentagens de ácido hialurónico de alto peso molecular tinham a menor taxa de degradação. Testes de viabilidade resultaram em valores mais elevados para os hidrogéis de 100% dextrino e 100% ácido hialurónico. Hidrogéis de dextrino e ácido hialurónico foram considerados como ligeiramente irritantes ao longo de 15 dias. Futuramente deverão ser realizados mais testes.

Este projeto resulta de uma parceria entre a Faculdade de Engenharia da Universidade do Porto, a Universidade do Minho e a empresa Biosckin.

Abstract

Tissue engineering is an emergent field that allows the treatment of several diseases. Mesenchymal stem cells can be used in these treatments since they have the ability to differentiate into several types of cells, including osteoblasts, adipocytes and chondrocytes. However, cellular expansion *in vitro* may be needed before its use in clinical applications in order to obtain the required amount of cells. During that period mesenchymal stem cells need to maintain an undifferentiated state. Hydrogels can be used as scaffolds due to their biocompatibility and high water content that promotes cell viability. Hyaluronic acid and dextrin hydrogels can be used as a platform to proliferate mesenchymal stem cells, due to their chemical and mechanical properties that mimic the extracellular matrix. These hydrogels were evaluated to determine the duration of the undifferentiated state of mesenchymal stem cells in these biomaterials.

Dextrin and hyaluronic acid hydrogels were produced with different types of hyaluronic acid and with different proportions. Their characterization was performed based on oxidation degree, gelation period and degradation rate. Preliminary viability tests were performed through a resazurin assay and a MTT assay, and using MG-63 cells. Finally, the hydrogels were implanted subcutaneously in mice and a histological analysis was performed through ISO 10993 Standard to assess biocompatibility. Results showed a lower gelation time for all the hydrogels and low degradation rates for mixed hydrogels with high contents of high molecular weight hyaluronic acid. Viability assays revealed high values for 100% hyaluronic acid and 100% dextrin hydrogels. Dextrin and hyaluronic acid hydrogels were found to be slight irritant during a 15 days period. Further testing should be performed.

This project is a partnership between the Faculty of Engineering of University of Porto, University of Minho and Biosckin.

Agradecimentos

Começo por agradecer ao Professor José Domingos Santos e ao Professor Miguel Gama por me terem proposto este tema e pela sua orientação e ajuda. Agradeço ainda o trabalho e a paciência constantes para fazer comentários e correções pertinentes de modo a aumentar a qualidade do projeto. Também agradeço à Professora Colette Maurício, à Dr.ª Irina Amorim e à Professora Maria Helena Fernandes pelas sugestões, correções e disponibilidade, mesmo durante o fim de semana.

Um enorme obrigada à Dina Silva pela disponibilidade e sorriso na cara e por me ter ajudado pacientemente em todas as etapas envolvidas neste projeto. Obrigada ainda pelas palavras de apoio quando as coisas não corriam bem. Agradeço também ao Tiago Valente pela companhia e animação sempre presentes e pelos ensinamentos partilhados. Rita Caseiro, obrigada também pela disponibilidade e sorriso em passar várias horas no microscópio a contar células iguais mas diferentes, mesmo depois de um longo dia de aulas só para que eu pudesse ter resultados a tempo. Agradeço também a todas as pessoas da Biosckin, do Laboratório de Tecnologia Enzimática e Biomateriais da Universidade do Minho e do departamento de Farmacologia da Faculdade de Medicina Dentária da Universidade do Porto pela companhia e pela ajuda dada.

Agradeço também aos amigos que fiz durante estes cinco anos com quem passei momentos inesquecíveis, dentro e fora da FEUP. Foram pessoas que me receberam de sorriso na cara sem esperar nada em troca, tendo-me apoiado nas fases mais difíceis. Obrigada também pela companhia durante as várias noites de estudo. Agradeço ainda à minha família pela animação constante e que tive que abdicar por vezes para trabalhar ou estudar. Obrigada pela vossa compreensão.

Por último, um obrigada especial aos meus pais e irmão a quem dedico este trabalho. Sem o seu amor incondicional e sem o seu apoio não seria possível para mim chegar a este ponto. Peço desculpa por terem aturado os meus momentos de irritação quando as coisas não corriam bem e um grande obrigada pela vossa compreensão e carinho.

"Optimism is an essential ingredient of innovation.
How else can the individual welcome change over security,
adventure over staying in safe places?"

Robert Noyce

Table of contents

List of figures

List of tables

Abbreviations

ADH	Adipic Dihydrazide
CL-HA	Crosslinked Hyaluronic Acid
Dex	Dextrin
DO	Degree of Oxidation
ECM	Extracellular Matrix
ETC	Ethylcarbazate
FBS	Fetal Bovine Serum
GAG	Glucosaminoglycan
HA	Hyaluronic Acid
HE	Hematoxilin-Eosin
MSC	Mesenchymal Stem Cell
MW	Molecular Weight
PEG	Polyethylene Glycol
RGD	Arginine-Glycine-Aspartic Acid
WJ	Wharton's Jelly

Chapter 1

Introduction

Tissue engineering is an emergent field for the treatment of several diseases as an alternative to allogenic and alloplastic transplants. This type of regenerative medicine can use cell transplantation and injection of growth factors or cells [1]. Stem cells can be used to treat wound healing, myocardial infarction, spinal cord injury or osteoarthritis, among other diseases, since they do not elicit an immunogenic reaction. According to the origin and potentiality of the cells, mammalian stem cells can be classified into two groups: embryonic stem cells and adult stem cells, which include mesenchymal stem cells (MSCs) [2]. MSCs are multipotent stem cells, able to differentiate into three main different cellular lineages: osteoblasts, adipocytes and chondrocytes [3]. The use of embryonic stem cells has several ethical controversies since their collection imply the destruction of a fetus. Therefore adult stem cells are emerging as a good alternative. However, cells must be propagated *in vitro* in order to obtain large numbers needed for biomedical applications [2].

Scaffolds play a major role in tissue engineering since they direct cellular processes based on its structural and biochemical properties. Different materials can be used according to the cell type, expected duration and microenvironment, and they determine several physical properties such as biocompatibility, biodegradability and mechanical stability [4]. The scaffold must also provide appropriate signals to direct cellular processes including cell adhesion and migration which can influence the survival of transplanted cells. The surface of the scaffolds can also be designed or functionalized with growth factors to control these processes [4]. Topographical patterns can also be introduced in order to orient cell growth, alter gene expression, and regulate the structure and the mechanical properties of the resulting tissue [4]. Several materials have been already investigated to produce scaffolds namely collagen, fibrin, alginate and hyaluronic acid (HA), for example [5].

1 Introduction

This project stems from the necessity to proliferate MSCs while preserving their undifferentiated state, until their differentiation is wanted for clinical use. Previous studies [6] reported that HA could maintain an undifferentiated state in human embryonic stem cells. Due to their physical and chemical characteristics, HA and dextrin (Dex) hydrogels will be produced in order to determine how long the undifferentiated state is maintained in this biomaterial. Physical and chemical tests will be performed to evaluate the cellular characteristics overtime.

Chapter 2

State of the art

This chapter presents the state of the art regarding the main subjects in this project: MSCs and hydrogels, including HA hydrogels and Dex hydrogels.

2.1 – Mesenchymal stem cells

Lately multipotent stem cells in adult tissue have received increased attention. MSCs have the ability to self-renewal and differentiate into several different types of cells namely osteocytes, adipocytes, chondrocytes, myocytes, cardiomyocytes and neurons (Figure 2.1) [2]. MSCs support hematopoiesis and increase the engraftment of hematopoietic stem cells after cotransplantation. Long-term culture of MSCs may result in senescence or spontaneous transformation [7].

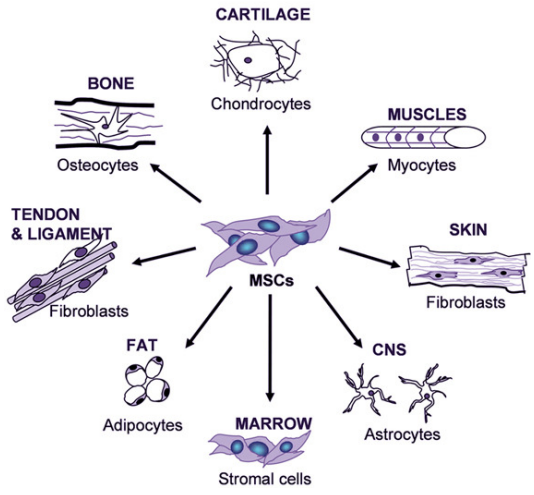

Figure 2.1. Different types of cells differentiated from MSCs [8].

MSCs are often identified by testing the differentiation potential of a culture into colony forming units which also indicates a proliferative capacity. In addition, the ability to adhere to tissue culture plastic and a fibroblast-like morphology are characteristics of MSCs. Different surface markers can be associated with these type of cells [9]. MSCs mainly express CD44s which is the standard form of CD44 whereas tumour cells are associated with the expression of several CD44 isoforms [10]. Astachov *et al.* [10] demonstrated that bone marrow-derived MSCs express toll-like receptors and this expression is upregulated in the inflammation zones.

However, despite all the advantages of using MSCs in tissue engineering, the procedure to isolate this type of cells from the bone marrow is very invasive. In addition, the differentiation potential of bone marrow-derived MSCs is age-dependent so alternative sources such as umbilical cord blood and umbilical cord could be advantageous. In addition to the non-invasiveness of these sources, they have higher availability and potential for autologous cell-based therapy. Umbilical cord blood appears to be a less frequent source for MSCs than umbilical cord [7].

MSCs also have the ability to reduce allogeneic lymphocyte proliferation *in vivo* and *in vitro* which influences the rejection of infused cells. Recently, several studies reported that MSCs express different molecules involved in the inhibition of T-cell proliferation and dendritic cell differentiation, and other molecules responsible for the induction of T-cell anergy and regulatory T-cell expansion. Therefore, it was hypothesized that MSCs may have a role in inducing tolerance in the host immune system [3].

MSCs can be isolated from several sources: periosteum, trabecular bone, adipose tissue, synovium, skeletal muscle, deciduous teeth, amniotic fluid, umbilical cord blood, and umbilical cord, among others. The umbilical cord contains two arteries and one vein surrounded by mucoid connective tissue known as Wharton's jelly (WJ) (Figure 2.2). MSCs can be isolated from either WJ or the umbilical cord vein, including perivascular regions. MSCs derived from the umbilical cord have no significant size differences and share the same surface markers as MSCs from other sources. Ishige *et al.* [7] successfully isolated MSCs from WJ, umbilical cord vein and arteries, and compared their proliferation and precursor potential. MSCs displayed similar fibroblast-like spindle-shaped morphology, with no significant differences relatively to the source. Over 90% of the cells exhibit positive surface antigenicity for CD13, CD29 (Integrin b1), CD73 (SH3), CD90 (Thy-1), CD105 (SH2; Endogrin), and HLA-ABC. 99% of the cells were negative for CD31, CD34, CD45, CD133, CD271, and HLA-DR. This way, there was no significant difference in the surface antigenicity profiles of WJ, umbilical cord arteries and umbilical cord vein. GD2 antigen was expressed in all parts of cells as it can be seen in Figure 2.3 [7].

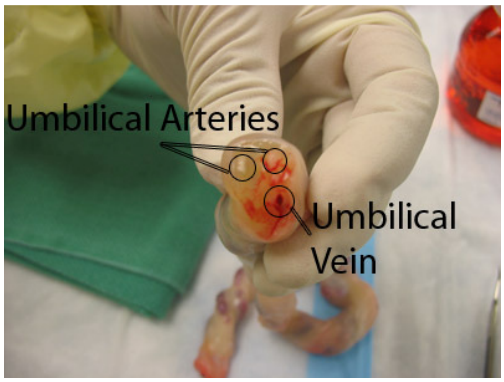

Figure 2.2. Cross section of the umbilical cord showing the umbilical vessels [11].

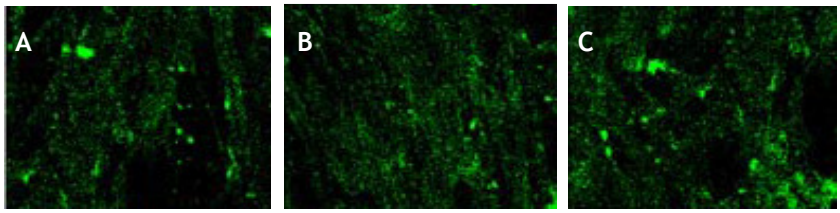

Figure 2.3. GD2 antigen expression in MSCs from three different sources: WJ (A), umbilical cord vein (B) and umbilical cord arteries (C) [7].

At early passages, MSCs are reported to be small in size and spindle-like in morphology, and exhibit high proliferation rate and great differential potential. However, after a long period of expansion, MSCs become large and flatten, and lose their ability to self-renew and differentiate. At early passages MSCs also express a low level of lineage-differentiation genes such as Pax6, Gata4, Cdx2, Stella or Nestin for ectoderm, endoderm, trophoectoderm, germline or neural lineages, respectively. These are highly expressed after a long period of expansion [2].

Ishige *et al*. [7] evaluated the proliferation potential of MSCs from WJ and the umbilical vessels. Results from a 9 days assay indicated that WJ and umbilical cord arteries exhibited, after 3 days, a significantly higher proliferative potential than umbilical cord vein-derived cells (Figure 2.4) [7].

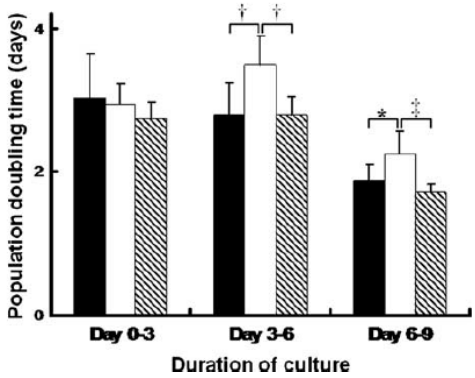

Figure 2.4. Doubling times of cell derived from WJ (black bars), umbilical cord vein (white bars) and umbilical cord arteries (hatched bars) [7].

Reactive oxygen species and other free radical emissions by cells and tissues are often considered as an indicator and a cause of aging *in vitro* and *in vivo*. However, in the case of MSCs, these reactive oxygen species are also involved in signalling, down-regulating proliferation and stimulating differentiation processes. In umbilical blood derived MSCs, superoxide radicals stimulate TGF-β1 which in turn stimulates colony forming units proliferation and osteogenic differentiation [9].

2.1.1 - Wharton's jelly

Umbilical cord is an extraembryonic formation that connects the placenta and fetus during pregnancy. It is covered by the umbilical epithelium, also known as amniotic epithelium, layered with cubic epithelial cells [3]. WJ was first described in 1656 by Thomas Wharton and is the primitive connective tissue of the umbilical cord, surrounding the umbilical vessels (Figure 2.5) [7]. It contains an abundant extracellular matrix (ECM) composed of sparse collagen fibers and an amorphous substance. The main function of WJ is to prevent torsion, compression and bending of the vessels, maintaining the blood flow between maternal and fetal circulations. WJ is rich in proteoglycans, such as HA, and two cell types: myofibroblasts and fibroblast-like cells. WJ expresses osteopontin, which is a regulator of hematopoietic progenitor cells and a major component of the hematopoietic stem cells' niche along with HA. Myofibroblasts have ultrastructural characteristics of both fibroblasts and smooth muscle cells and play a role in fibrogenesis and contraction. Fibroblast-like cells constitute MSCs so they are multipotent, grow robustly *in vitro*, can be deep-frozen for long term storage, and maintain a morphology similar to fibroblasts during culture [3].

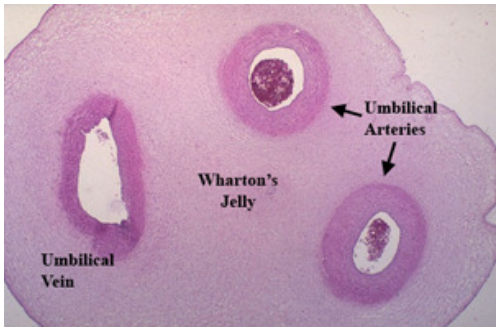

Figure 2.5. Cross-section of the umbilical cord showing WJ and the umbilical vessels [12].

Recently, more attention has been given to WJ as a potential new source of MSCs. However, the efficient isolation of cells that truly express MSCs characteristics has been controversial. Nanaev *et al*. [13] reported that cells close to the amniotic surface have higher capacity to retain the ability to proliferate whereas highly differentiated and non-proliferating fibroblasts were located in closer proximity to the vessels. In other hand, Baksh *et al*. [14] showed that CD146-positive cells, including MSCs, were not distributed in WJ but

in the perivascular region of the vein. The CD146 marker can be used to distinguish the multidifferentiation potential of different cell populations. WJ-derived cells show a phenotype closely resembling that of MSCs derived from bone marrow. They express CD10, CD13, CD29, CD44, CD49e, CD73, CD90, CD105, CD166 and HLA class I. In addition, similar to bone marrow-derived MSCs, WJ-derived cells lack expression of hematopoietic markers such as CD34 and CD45 [3]. Ishige *et al*. [7] reported that cells derived from WJ were unable of undergoing osteogenic differentiation until day 49 of culture, despite the detection of osteopontin transcripts. Alkaline phosphatase activity also appeared defective in WJ and in umbilical cord vein cells. However, relatively high alkaline phosphatase activity was present in umbilical cord arteries-derived cells, even in non induction medium. This suggests that cells derived from umbilical cord arteries may retain characteristics of the arterial wall since alkaline phosphatase activity is specific to arterial segments but not to venous segments. In addition, Mitchell *et al*. [15] reported that pre-chondrocytes were present in explants WJ cultures. Ishige *et al*. [7] differentiated the cells derived from WJ into chondrocytes and observed that the cell populations derived from WJ and the umbilical vessels appeared to consist of different proportions of multipotent stem cells, even though no major differences in antigens profiles was found [7]. Cells derived from these sources exhibited strong positive staining by toluidine blue for ECM, suggesting that new ECM was induced by chondrogenic differentiation (Figure 2.6). WJ-derived cells can be differentiated into chondrocytes-like cells if cultured in a medium supplemented with ascorbic acid, transferrin, dexamethasone, retinoic acid and TGF-β3 for up to 46 days [3]. In their experiments, Ishige *et al*. [7] could not demonstrate the differentiation ability derived from a single cell maybe because it could already enter in a senescence state during the explants migration or the environmental culture conditions were not appropriate for expansion. However, the investigators claim that umbilical cord-derived cells with the typical phenotypes for MSCs might be equivalent to bone marrow-derived cells. MSCs can also differentiate in neuron-like cells and cardiomyocytes [7].

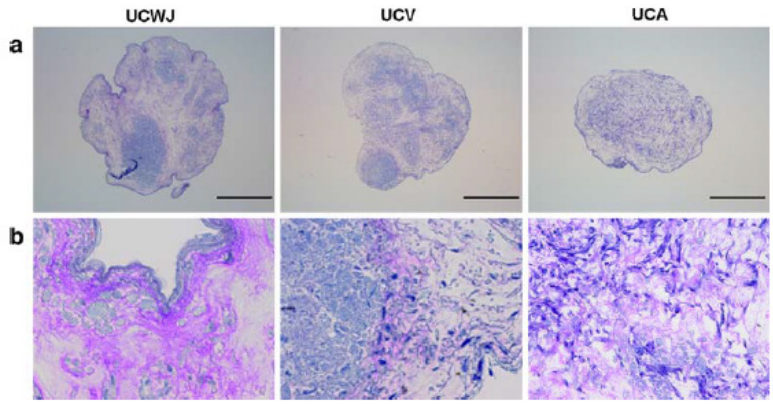

Figure 2.6. Chondrogenic differentiation potential of cells derived from WJ (UCWJ), umbilical cord vein (UCV) and umbilical cord arteries (UCA). Results from toluidine blue staining in cells induced with chondrogenic differentiation medium with different magnification: x10 (a) and x40 (b). Bar = 1mm [7].

Iacono *et al*. [3] reported that WJ-derived cells express mesodermal markers (vimentim and α-smooth muscle actin), endodermal markers (Gata-4, Gata-5, Gata-6 and HNF4-α), and neuro-ectodermal markers (nestin, neuron specific enolase and glial fibrillary acid protein) which indicates that these cells can differentiate towards different mature cell types derived from all three germ layers. WJ-derived cells can be cultured in a medium supplemented with factors inducing osteogenic differentiation. Consequently, they can express osteonectin, osteopontin, periostin and runx2 genes and proteins. The differentiation into an osteoblast can be confirmed also by histological stains such as Alizarin Red and Von Kossa which allow the visualization of calcium deposits in the ECM. In addition, this type of cells can be induced with adipogenic induction medium and develop lipid vacuoles that can be stained using Oil Red O. They also express proteins namely adiponectin, leptin and PPAR [3].

Seeding density is an important factor in the presence of chondrogenic medium and influences the chondrogenic potential. Wang *et al*. [16] cultured MSCs from WJ in a chondrogenic medium within PGA scaffolds for one month at different seeding density: 5, 25, and 50 million cells/ml. Higher density groups showed more glucosaminoglycans (GAGs) and collagen type I and II than in a lower density group. Mechanical integrity was also higher in the higher density group. This indicates the potential for chondrogenic differentiation and the importance of higher seeding density in order to promote biosynthesis and mechanical integrity for a possible application in fibrocartilage tissue engineering [3].

2.1.2 – Maintenance of the undifferentiated state of mesenchymal stem cells

One limitation to the use of MSCs in clinical applications is their tendency to lose potency for proliferation and differentiation when cultured *in vitro* which is influenced by donor age, plating density, serum composition, and passage time. This way, methods to maintain the long term multipotency of these cells would significantly improve their use in clinical settings [17].

MSCs must balance self-renewal and differentiation, and complex regulatory mechanisms are required to maintain stem cells undifferentiated and to control their subsequent differentiation and proliferation. It has been reported that the mesenchymal phenotype can be maintained under optimal culture conditions. Toyoda *et al*. [18] reported that the inhibition of the p16/Rb pathway is sufficient to extend the life span of cells in cultures of bone marrow-derived cells. This pathway leads to senescence and can be inhibited by inducing the human papillomavirus type 16 E7 gene, allowing the long term cultivation of bone marrow-derived cells. MSCs can also have their life span extended via retroviral transduction of human telomerase reverse transcriptase. In this process, cell characteristics remain unaffected, including the surface markers and the growth factor reactivities of transduced cells. Toyoda *et al*. [18] also reported that excessive stimulation by growth factors can be a cell senescence inducer so this factor needs to be taken into account.

Stem cells are reported to survive in a hypoxic environment and this condition influences the maintenance of multipotency and extension of survival. However, the degree and duration of hypoxia described in the literature vary greatly and may result in opposite effects on the proliferation and differentiation capacities of MSCs [19]. Grayson *et al*. [20] studied the long term effect of human MSCs cultured under low O_2 tension (2% O_2) and showed improved survival and increase in adipocytic and osteogenic differentiation capacity. In another study, Basciano *et al*. [19] compared cultured human MSCs derived from bone marrow in normoxia (21% O_2) or hypoxia (5% O_2) for up to passage 3. They observed that cells under low O_2 tension were more undifferentiated than cells cultured in normoxia. In addition, hypoxia inhibited the expression of genes involved in DNA replication and cell division at passage 0. However, in later passages, cells expanded faster. In this study, cultured cells displayed a typical MSC profile with stable phenotype overtime and no significant phenotypic differences between hypoxic and normoxic conditions were found. Hypoxia also inhibited the biosynthesis of mitochondria in 50% to 75% of cells. The investigators also differentiated the MSCs in both conditions and observed that hypoxic cells were more prone to osteogenic differentiation than normoxic cells and that the expression of alkaline phosphatase was stronger in hypoxic MSCs. This study reflects the capacity of hematopoietic and stromal stem cells to adapt to hypoxia in culture. Hypoxic MSCs are also more adhesive [19].

MSCs express Oct4 or Nanog, which can be increased under specific conditions such as serum deprivation. These are pluripotency genes that constitute the core regulatory network that suppresses differentiation-associated genes, thereby maintaining the pluripotency of the cells. Expression of these genes is restricted to plutipotent cells and is downregulated upon differentiation. Chih-Chien *et al*. [2] reported that Oct4 and Nanog levels were higher in early passages, as expected, and in hypoxic cultures. In addition, the protein levels of Oct4, the isoform associated with pluripotency, were maintained over long-term cultures in hypoxia. Knockdown of Oct4 or Nanog induced an increase in the expression of Pax, Gata4, Gata6, Sox17, and FoxA2 at early passages in MSCs cultured in hypoxic conditions which indicates spontaneous differentiation. These results suggest that Oct4 and Nanog prevent spontaneous differentiation in MSCs. In addition, the overexpression of Oct4 and Nanog in MSCs enhances the proliferation rate and differentiation potential while inhibiting spontaneous differentiation during expansion under normal culture conditions [2].

In another study, Zhang *et al*. [17] used microcontact printing of alkanethiolates on gold as a model system for culturing MSCs in patterns. Results showed that by restricting cell spreading, the MSC phenotype was maintained, with higher levels of stem cell markers, even after the removal of the patterns. The differentiation potential was not affected. When confined to the microislands so created, MSCs did not divide because DNA synthesis was restricted. MSCs are also characterized by positive expression of markers such as CD31, CD44, CD90, Stro-1, endoglin, CD106, and CD166. In this study, Stro-1 and endoglin were observed to have higher expression during early passages compared to senescent passages and Stro-1 has been shown to be downregulated in prolonged cultures. When MSCs are confined to small

islands express higher levels of endoglin and Stro-1 compared to cells cultured on non-patterned surfaces, even after the cells are removed from the islands after a week and cultured on tissue culture plastic for up to 16 days [17].

Gerecht *et al*. [21] also reported the maintenance of the undifferentiated state of human embryonic stem cells in HA hydrogels in the presence of conditioned medium from mouse embryonic fibroblast feeder layers until soluble factors are introduced to direct cell differentiation. During development, cellular interactions with HA are mediated by CD44 which is highly expressed *in vitro* by human embryonic stem cells [6]. Since MSCs also express CD44, it may be possible for HA hydrogels to control their undifferentiated state [3].

The main requirement when culturing MSCs is to recreate the specific native tissue/organ milieu of the cell's origin; hence the choice of HA and Dex hydrogels, which are going to be used in this project.

2.1.3 – MG-63 cells

MSCs differentiate in several types of cells, including cells from the osteogenic lineage. In many *in vitro* studies of the interactions between cells and biomaterials, immortalized cell lines have been used instead of primary cells like MSCs due to mainly practical reasons: immortalized cell lines are easier to acquire than primary cells and grow *in vitro* for an indefinite number of passages [21]. To test the differentiation profile in biomaterials, human osteoblast-like cell line MG-63 can be used as cellular prototype since they have the capacity to undergo osteoblastic differentiation in response to an osteogenic environment [21][22]. This cell line was originally isolated from a human osteosarcoma (the most common primary solid tumour of bone in children and young adults) and has been well characterized and largely used in biocompatibility tests [23].

MG-63 cells produce collagen type I and express ALP activity which is further enhanced by dihydroxyvitamin D_3. This also enhances the production of osteocalcin and other markers of osteoblast function. The interaction between dihydroxyvitamin D_3 and TGF-β appear to induce differentiation of MG-63 cells into the ECM maturation stage without continued differentiation into the mineralized state, presenting a similar behaviour as human explants bone cells [24]. Unlike osteoblasts, MG-63 cells do not vary their size depending on cell density. They are oval to spindle-shaped, without branching processes [25].

Comparing MSCs and MG-63 cells, they both express exogenous $p75^{NTR}$ protein which is an important neuronal signalling molecule that interacts with numerous ligands and coreceptors, promoting cell proliferation and osteoblast differentiation [26]. MG-63 cell adhesion is significantly inhibited by function-blocking antibodies against the αv and α5 integrin subunits that are involved in binding to fibronectin. However, MSCs use αv-containing integrins to adhere to fibronectin [21]. Regarding surface markers, both MSCs and MG-63 cells highly express CD90 and CD44 [27].

2.2 – Hydrogels in Tissue Engineering

Tissue engineering takes advantage of scaffolds to direct cellular processes, hence the choice of its structural and biochemical properties is decisive. Hydrogels have been used in clinical applications, such as drug delivery systems, tissue replacements, immobilization of proteins and cells, due to their high water content that promotes cellular viability since they are mechanically and structurally similar to the ECM of most biological tissues. In addition, hydrogels are highly customizable and biocompatible [28]. However, their tunable properties can influence the final results and are not always reported. This includes the hydrogel chemistry, the type of polymerization and the total polymer content, which will influence how transplanted cells react to hydrogel encapsulation. Hydrogel biocompatibility is improved when its mechanical properties are matched those of the host tissue [29][30].

Injectable hydrogels can be maintained in the liquid state before injection and harden after transplantation *in vivo*. The hydrogel allows the filling of irregular defects, decreases the risk of implant migration and minimizes surgical defect to the size of a needle. In addition, the hydrogel can be incorporated with therapeutic factors and cells [31]. Hydrogels can also be stimuli-sensitive and respond to pH, temperature, electric field, glucose and antigens, among others. This way the hydrogel can have a controlled drug release due to volume changes [30].

Hydrogels are composed of hydrophilic polymer chains and can be fabricated using natural or synthetic materials namely HA, collagen and Dex.

2.2.1 - Hyaluronic Acid

HA (Figure 2.7) is a linear polysaccharide consisting of alternating 1,4-linked units of 1,3-linked glucoronic acid and N-acetylglucosamine. This oligosaccharide adopts three-dimensional structures in solution with extensive intramolecular hydrogen bonding, restricting the conformational flexibility of the polymer chains and inducing distinctive secondary and tertiary interactions [32]. HA has several desired properties that can be used for application as a biomaterial in tissue engineering. It is a major intracellular component of the umbilical cord, synovial fluid of joints, cartilage and vitreous fluid of the eye, among others, and is synthesized at the inner wall of the plasma membrane by cells of mesenchymal origin [4][30][33]. HA can be synthesized by three types of HA synthase (HAS1, HAS2 an HAS3) which are located in the cell membrane and, after production, is immediately extruded out of the cell into the ECM where it interacts to provide mechanical support [33].

GAGs have a unique water binding ability due to the highly negative charge on the molecular chain [31]. This way, they can absorb large amounts of water and expand up to 1000 times in volume, forming a loose hydrated network. Due to this fact, HA acts as a space filler, lubricant, and osmotic buffer in the native ECM. This hydrated HA network controls the

transport of water, restricts the movement of pathogens, plasma proteins and proteases, and maintains the viscoelasticity of the connective tissues [33].

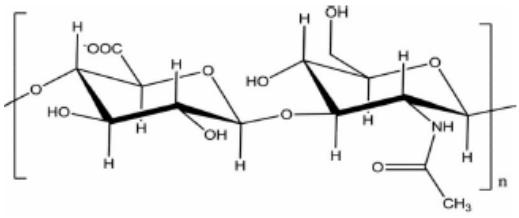

Figure 2.7. Basic chemical structure of HA [33].

HA exists as a high molecular weight (MW) polymer and forms the backbone of proteoglycans in the ECM. It differs from synthetic polymers such as polyethylene glycol (PEG) since it is biologically active, playing an important role in structure, lubrication, cell differentiation, cell migration, cell proliferation, and cell growth since cellular interactions occur through cell surface receptors such as CD44, RHAMM and ICAM-I [1][33]. HA interacts with these surface receptors to activate various signalling pathways such as c-Src, Ras and mitogen-activated protein kinases (Figure 2.8) that direct cell functions [33]. It also influences biological processes including morphogenesis, wound repair, and metastasis [1][4]. Inflammation can also be mediated by HA due to its ability to inhibit macrophage migration and aggregation, and to prevent the immune complex from adhering to polymorphonuclear cells. HA influences wound healing since it usually increases at scarless fetal wounds due to the reduced expression of proinflammatory cytokines (IL-1 and TNF-α) which are responsible for the down regulation of HA synthesis. HA expedites the delivery of solutes and nutrients due to its high water absorption capacity and its ability to stimulate inflammatory signals for wound healing. HA also improves cell migration and proliferation which are essential for this process [33].

HA degrades in the presence of hyaluronidases and free radicals [30]. Hyaluronidase degradation of HA results in the cleavage of internal α-*N*-acetyl-D-glucosaminidic linkages, producing fragments with *N*-acetylglucosamine at the reducing terminus and glucuronic acid at the nonreducing end. The networks decrease in size during degradation and exposure to hyaluronidase due to surface erosion, and attraction between positively charged groups produced during degradation and the negatively charged carboxylic acid groups of HA [5]. The degraded species are internalized by cells and degraded in lysossomes or transferred to the circulation and then cleared by the drainage systems such as liver, lymph nodes or kidneys. The half-lives of HA in biological tissues range from minutes in the blood to hours or days in skin and joints. However, this material is attractive for the fabrication of scaffolds since it is biocompatible, biodegradable, bioactive, non-immunogenic and non-thrombogenic. In physiological solutions, HA assumes an expanded random coil structure [33]. In addition, the rate of degradation depends on the hydrophobicity of the crosslinker used: increased hydrophobicity results in less degradable hydrogels [32]. HA degradation products appear to

have different biological functions from the native high MW polymer. Oligosaccharides of less than 20 disaccharides have been shown to be angiogenic and low and intermediate MW HA stimulate gene expression in macrophages, endothelial cells, eosinophils and certain epithelial cells. In addition, HA degradation products contribute to scar formation, especially if hyaluronidase is added to stimulate degradation. However, high MW HA promotes cell quiescence and supports tissue integrity. Under physiologic conditions, HA exists as a high MW polymer but following tissue injury, HA fragments of lower MW accumulate [34].

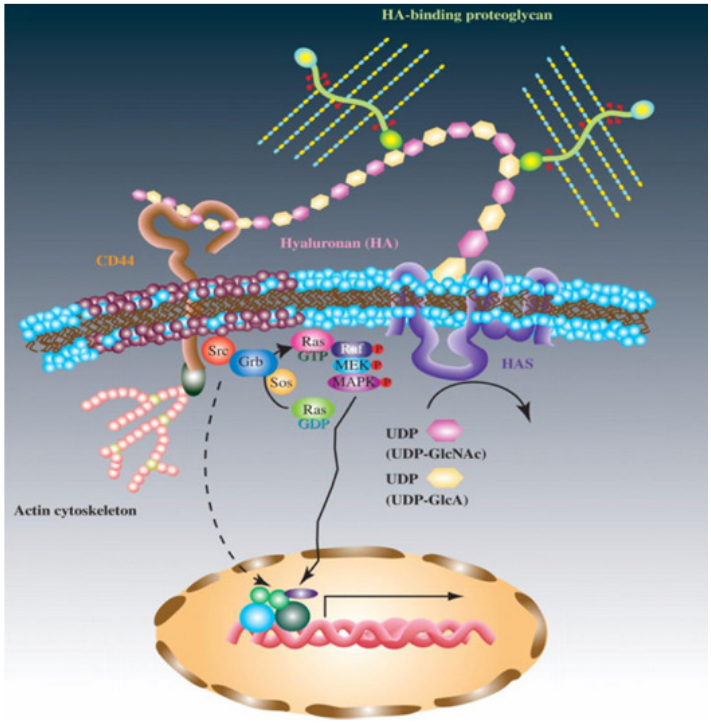

Figure 2.8. Signaling mechanism of HA [34].

HA is highly expressed in tumours and is a main component of the microenvironment of cancer cells. In addition, on the cell surface this GAG directs the metastasis of tumour cells by altering its biological activity and triggering the TGF-β, Rho GTPase, and FAK pathways through interactions with cancer cells surface receptors. In tumour sites, HA facilitates migration of invasive tumours through the expansion upon hydration and interaction of HA through specific cell surface receptors. HA oligomers encourage angiogenesis and induce inflammatory cytokine production that activates signalling mechanisms for cancer progression. This way, HA and hyaluronidase levels influence tumour progression and angiogenesis. In addition, HA coating around tumour cells protects them against the immune system, as explained previously [33].

It was observed that cellular interactions between chondrocytes and HA help the organization of the ECM of cartilage and retain proteoglycans within the cartilage. HA also stimulates the chondrogenic differentiation of MSCs and the proteoglycan production through its interaction with the chondrocytes [33].

For clinical applications and cosmetics, high MW HA (usually more than 1MDa) can be produced in large quantities with high purity by bacterial fermentation. Low MW HA can also be produced by γ irradiation or enzymatic degradation. Chemoenzymatic processes can be used to control molecular size distribution [33].

Soluble HA has been used in several clinical applications but native HA is not useful as a biomaterial due to its poor mechanical properties; also, rapid degradation and clearance *in vivo* limit its applications. In order to improve its mechanical properties HA can be combined with other materials such as collagen, be chemically modified or even crosslinked to form hydrogel. Chemical modification of HA usually involves the carboxylic acid and/or the alcohol groups of its backbone. The carboxylic acid groups can be modified by esterification and crosslinked via dihydrazide, dialdehyde or disulfide crosslinkers [4]. Comparing crosslinked HA with the native one, the first exhibit more robust mechanical properties and is less susceptible to enzymatic degradation. Covalent crosslinking of native HA can require toxic reagents (such as EDC) and harsh conditions that are not suitable for cell and protein encapsulation. So, for tissue engineering applications, the synthesis of HA hydrogels should be chemo-selective and occur under physiological conditions without creating any toxic by-products [33]. Prestwich *et al*. [32] produced HA hydrogels using adipic dihydrazide (ADH) as a crosslinking agent (Figure 2.9) and described them as possessing good biocompatibility. The hydrazide moieties are nucleophilic at low pH (3.0 to 4.75), leading to efficient coupling of the hydrazide to the carboxylic acids of the glucuronic acid units of HA. Linkers containing disulfide bridges can be introduced into the gel formation process to incorporate a way to unlink the gel. This type of gels can be reduced with thiols, hydrides, and phosphines back to sol form [32].

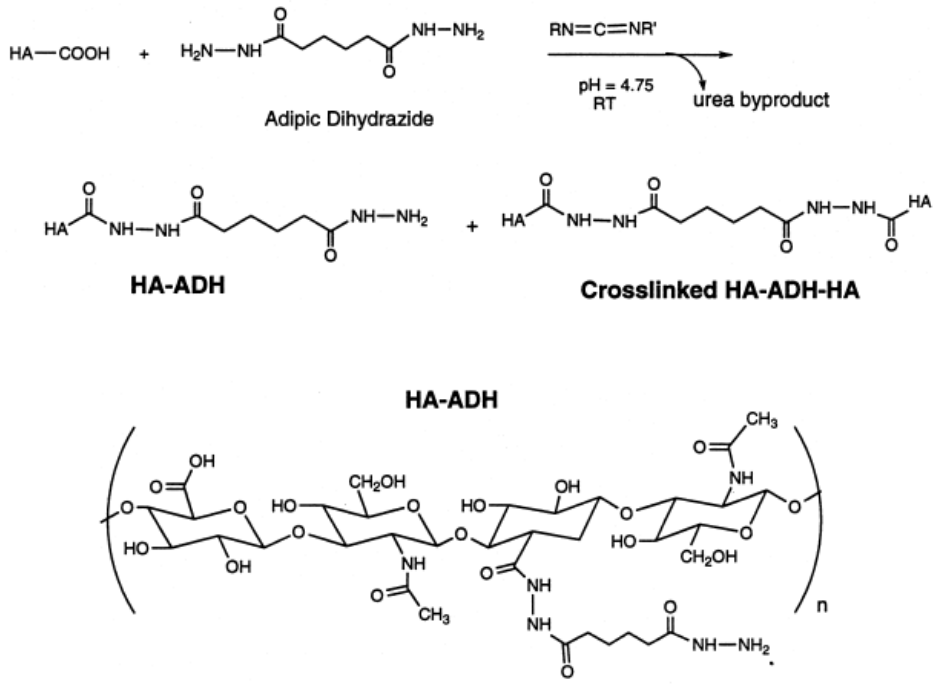

Figure 2.9. Functionalization and crosslinking of HA with ADH [32].

To regulate cellular interactions with hydrogels, cell adhesion sites can be introduced to HA by modification with the integrin binding peptide Arginine-Glycine-Aspartic Acid (RGD) or by coating them with adhesion proteins including collagen, laminin and fibronectin. Irradiation with ultraviolet light can also induce surface modifications that promote cell adhesion [4]. In another study, Burdick *et al*. [5] used HA with MW ranging from 50 to 1100 kDa modified with methacrylic anhydride and photopolymerized into networks and observed compressive moduli up to 100 kPa, swelling ratio from 8 to 42, and degradation times from less than 1 day up to 38 days in the presence of 100 U/mol of hyaluronidase, with macromer concentrations from 2 to 20 wt% (Figure 2.10). Biological functionalities can be incorporated into HA gels through the coupling of cytokines and therapeutic drugs, enabling the encapsulation of cells during gelation. The gelation kinetic should be fast enough to allow *in situ* cell encapsulation for the fabrication of 3D cell/gel constructs or *in vivo* hydrogel formation in a minimally invasive injectable manner [33].

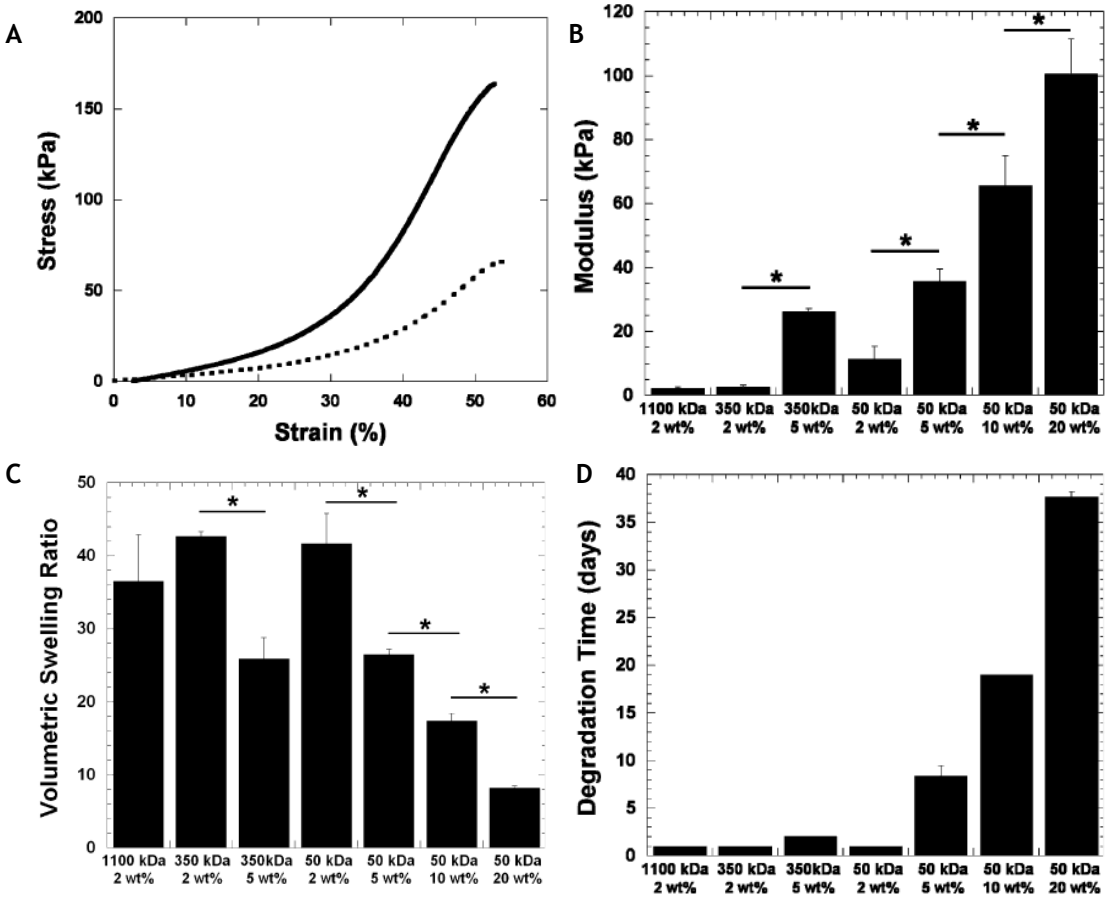

Figure 2.10. Mechanical properties of HA hydrogels produced. A. Representative stress versus strain plots fabricated from 10 (solid) and 5 (dotted) wt% macromers (50 kDa methacrylated HA). B. Compressive modulus for various HA networks at equilibrium swelling. C. Equilibrium volumetric swelling ratio for photocrosslinked HA networks with variations in macromer MW and concentration. D. Time for complete degradation of HA hydrogels in 100 U hyaluronidase/ml of PBS, where the hyaluronidase was replenished every other day throughout degradation. The compressive moduli and the swelling ratios are statistically different between the different macromer concentrations for each MW methacrylated HA [5].

Aurand *et al.* [29] studied the polymerization and degradation rates of hydrogels produced with different concentrations of HA and PEG and results showed that polymerization time decreased as HA and PEG concentrations both increased (Figure 2.11.A). Results also showed that hydrogels with greater concentrations of both materials had slower degradation. In addition, at higher PEG contents (1.8% to 3.0%), degradation rate was dependent on the HA content of the hydrogel (Figure 2.11.B) and changes in compressive modulus were driven mainly by the HA concentration [29].

Traditional HA-based hydrogels are macroscopic networks consisting of randomly interconnected HA chains. Drug molecules encapsulated in the network without any covalent linkage are released rapidly due to relatively large pore size. HA hydrogels with micro or nanopores can also be produced. These exhibit tunable size, large surface area, abundant interior space and addressable functional groups, allowing the encapsulation of active compound and control of their release. The water-filled interior also prevents severe aggregation of the drug and is suitable for the physical association and covalent conjugation of therapeutic agents. In addition, these HA hydrogels are unable to induce cells to regenerate architecturally complex healthy tissue [33].

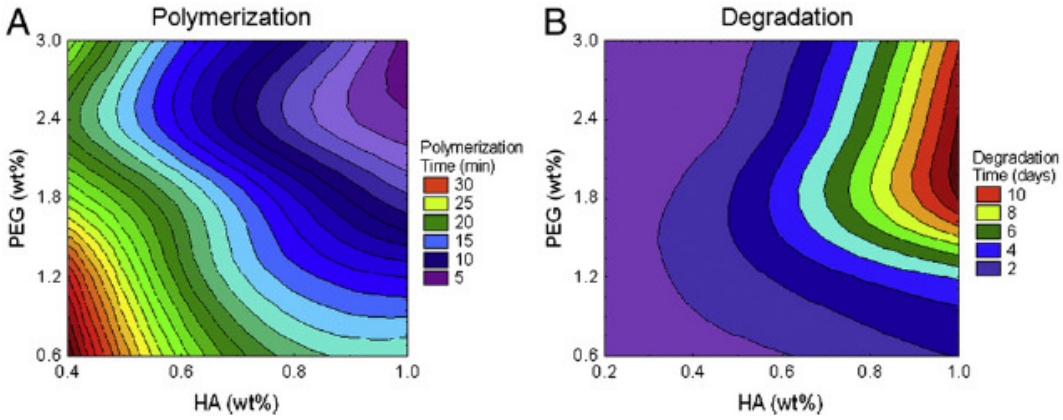

Figure 2.11. Physical properties of the hydrogel. Polymerization and degradation rates were determined *in vitro*. A. Polymerization rate measured in minutes. B. Degradation rate of hydrogels submerged in hyaluronidase solution measured in days [29].

HA-mediated signals are transmitted through cell surface receptors that are also expressed in MSCs: CD44, RHAMM (receptor for HA mediated motility) and the toll-like receptor 4. CD44 is the main receptor for HA and is one of the specific markers for MSCs. CD44 is a cell surface transmembrane protein that mediates cellular interactions and cell-ECM interactions, and is expressed by several cells and tissues. It regulates different biological functions such as cell-cell adhesion, pericellular matrix assembly, cell migration, HA endocytosis and tumour cell metastasis. Although CD44 proteins are encoded by a single gene, cells that display CD44 express some heterogenic isoforms of this receptor due to posttranslational modifications and to alternative splicing of ten variant exons in the cell membrane vicinity at the proximal region of the extracellular domain. The cytoplasmic tail of

CD44 does not contain actin-binding sites, and its interaction with the cytoskeleton is mediated by cytoskeleton-associated proteins such as merlin and ankyrin among others. HA also influences the integrity of the cytoskeletal structures since the cytoplasmatic domain of CD44 is required for HA binding and its internalization. The affinity of CD44 to this GAG requires a very specific glycosylation pattern and helical folding of the HA-binding domain of CD44 [10].

RHAMM is another HA receptor that is critical for cell motility and focal adhesion turnover. Similarly to CD44, RHAMM also has multiple isoforms. It is located at the cell membrane and has no transmembrane or cytoplasmic domains. However, Assman *et al*. [35] reported that it is present in the cytoplasm where RHAMM interacts with microtubules and actin filaments. This receptor is activated during cell migration and its inhibition during embryogenesis causes loss of pluripotency and cell viability in human embryonic stem cells. Further experiments revealed that in CD44 knockout mice, the RHAMM gene compensates for the loss of CD44 by supporting up-regulating genes associated with CD44. In addition, toll-like receptors for HA are involved in the signalling of bone marrow-derived MSCs and are used to detect inflammation and initiate host defence response mechanisms [9].

2.2.2 - Dextrin

Dex (Figure 2.12) is a polymer composed of α-(1→4) D-glucose units produced by partial hydrolysis of starch using acids, enzymes or a combination of both. This material is used in several applications including adhesives, and in food industry and textiles [37]. Dex is already used clinically as a peritoneal dialysis solution [38][39]. In addition, due to its biocompatibility and biodegradability, Dex hydrogels can be used in tissue engineering. Systems based on linear Dex have been found to promote cellular growth [37].

This biocompatible polymer can be hydrolyzed enzymatically by α-amylase which is responsible for *in vivo* degradation of Dex [28][39]. In Dex hydrogels, degradation occurs mainly by bulk erosion and it is characterized by nonlinear degradation profile with an increasing pore size. This variation affects the swelling of the hydrogel, the diffusion of molecules, and the delivery of cells when the hydrogel is used for cell encapsulation [28].

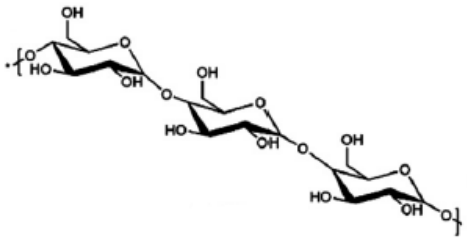

Figure 2.12. Basic chemical structure of Dex [36].

The production of starch-based hydrogels can include one or two-step free radical graft polymerization of hydrophilic vinyl monomers in the presence of a crosslinker. However, this technique presents some disadvantages such as the use of catalysts which are difficult to remove from the reaction mixture and could significantly increase the toxicity of the material [36].

Previous studies evaluated cell spreading of cells growing on starch-based hydrogels and revealed differences in cell morphology. Cells appeared round and clustered but viable when grown in hydrogels [40]. Moreira *et al.* [38] developed a strategy to functionalize a Dex-based hydrogel using a RGD-sequence and results with fibroblasts showed that in this condition the cells are uniformly distributed while exhibiting the characteristic fibroblast morphology (Figure 2.13). These results indicate that cell spreading occurred. Moreira *et al.* [38] also performed MTS assays to analyse cell adhesion and results (Figure 2.14) indicate that Dex hydrogels have a 50% adherent cells. Moreira *et al.* [38] also evaluated cell proliferation and reported that there is a moderate cell growth on non-activated hydrogels, and that the presence of a starch-binding molecule and a RGD sequence do not lead to a significant increase in the proliferation rate, despite its effect on cell morphology [38].

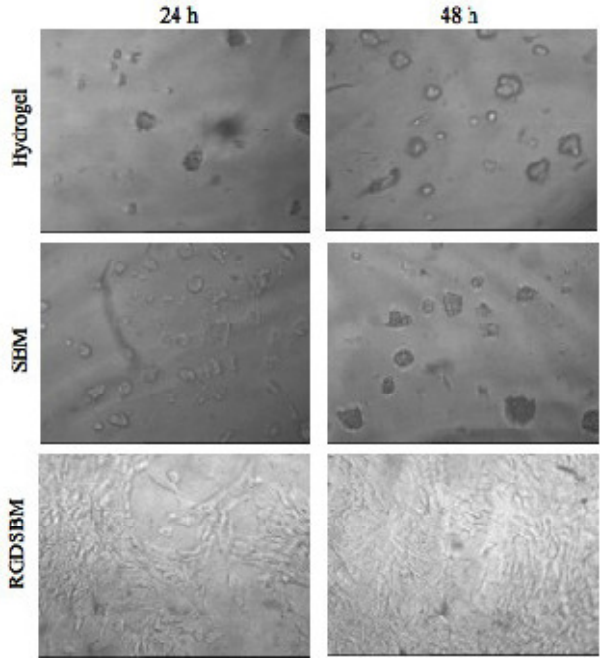

Figure 2.13. Microscopic analysis of the fibroblasts cultivated on Dex hydrogels without recombinant proteins, coated with a starch-binding molecule (SBM), and coated with a starch-binding molecule and a RGD sequence (RGDSBM) with different incubation times [38].

Dex hydrogels can be obtained by crosslinking following oxidation. The oxidized dextrin is characterized by their oxidation degree which consists on the quantification of aldehyde groups. The oxidation reaction is characterized by the specific cleavage of the C2-C3 linkage of glucopyranoside rings, yielding two aldehyde groups per glucose unit. The degree of oxidation (DO) can be easily controlled by the relative quantity of sodium periodate used,

yielding free aldehyde groups to create covalent linkages with reticulating molecules or cellular adhesion binding peptides. Dex solutions can only be produced with concentrations less than 30% (w/v). Above that value, the solution is extremely viscous and very difficult to homogenize. This way, this concentration is considered the threshold of Dex solubility in phosphate buffer pH 6.0 [28].

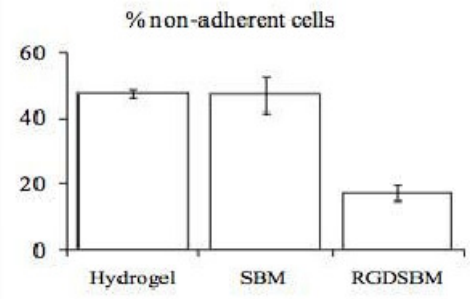

Figure 2.14. MTS analysis using Dex hydrogels without recombinant proteins, coated with a starch-binding molecule (SBM), and coated with a starch-binding molecule and a RGD sequence (RGDSBM) [38].

The DO and the concentration ADH, which is a reticulating molecule, influence the gelation periods, as it can be seen in Table 2.1. The DO was calculated as the molar ratio of sodium periodate per initial glucose unit in Dex. The ADH concentration was calculated in molar base, taking into account the number of glucose residues in the original Dex. Results show that gelation times decrease with increasing DO. It is reported that a DO above 40% yield very viscous solutions that react promptly with ADH, preventing good homogenization and resulting in mat and brittle hydrogels. This way, 40% is the desired DO for Dex hydrogels. In addition, an increased concentration of ADH results in a proportionally higher compressive modulus for cross-linked Dex hydrogels as it can be observed in Figure 2.15 [28].

Table 2.1 - Gelation periods estimated for Dex hydrogels with different ADH concentrations. Gelation times correspond to more than 1h (+++), less than 30min (++) or less than 1min (+) [28].

Degree of oxidation (%)	**ADH (%)**		
	5	15	30
25	+	+	+
32.5	++ (~30 min)	++ (~10 min)	++ (~15 min)
40	++ (~2 min)	+++	+++
50	+++	+++	+++

Molinos *et al*. [28] also characterized biocompatibility for Dex hydrogels and it was observed that the products of the hydrogels degradation can be potentially cytotoxic and cellular death is observed when the degradation products of Dex are in direct contact with

cells. This is due to mechanical pressure or decreased oxygenation and nutrient diffusion caused by the products sedimentation. However, since there is a rapid reabsorption and excretion *in vivo*, cytotoxicity decreases for *in vivo* assays [28].

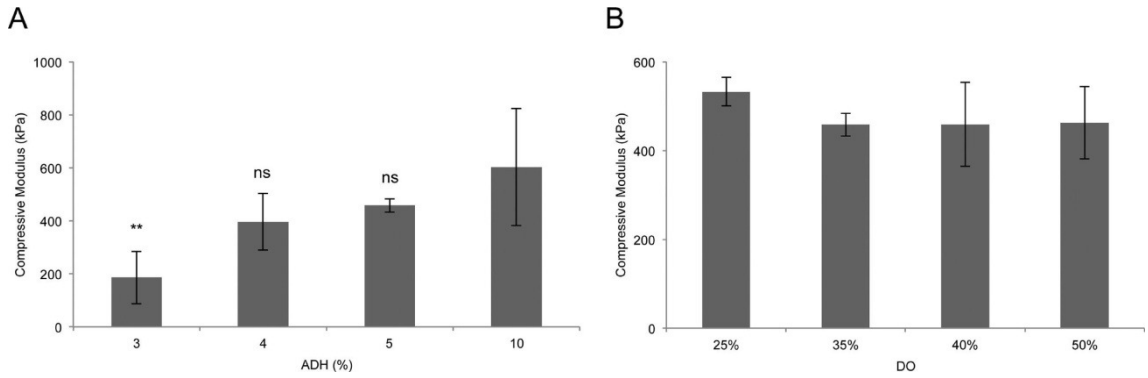

Figure 2.15. Compressive modulus of crosslinked Dex hydrogels as a function of ADH concentration (A) and DO (B) of Dex [28].

Chapter 3

Materials and Methods

All reagents used were purchased from Sigma-Aldrich, unless stated otherwise. Tackidex Dex was obtained from Roquette and Hyasis® Link Hyaluronic Acid (CL-HA) (0.7 - 1 MDa) was obtained from Novozymes Biopharma. Hylumed high MW HA (0.8 – 2 MDa) was obtained from Genzyme Corporation and low MW HA (<10 kDa) was obtained from Lifecore Biomedical. Oxidized Dex was prepared according to Molinos *et al*. [28] and the three types of HA followed the same protocol.

3.1 – Production of hyaluronic acid and dextrin hydrogels

3.1.1 – Dextrin preparation

Aqueous solutions of Dex (2% w/v) were prepared. Dex was oxidized with sodium *m*-periodate solution at room temperature, in the dark and with stirring for 20h, in order to obtain a theoretical DO of 40%. Sodium periodate can be used as oxidizing agent in order to create the aldehyde function which further crosslinks through ADH to form the hydrogel [31]. The oxidizing reaction was stopped by adding an equimolar amount of diethyleneglycol to reduce any unreacted periodate. The resulting solution was dialyzed for 3 days against deionized water using a dialysis membrane with a MW cut off of 1000 Da and then lyophilized for 10 days using the freeze-dryer Scanlaf Scanvac 100-9 Pro Alpha 2-4.

3.1.2 – Hyaluronic acid preparation

Aqueous solutions of the different types of HA (1% w/v) were prepared and an equimolar amount of sodium *m*-periodate was added at room temperature, in the dark and with stirring for 24h to oxidize the solution, in order to obtain a theoretical DO of 100%. The oxidizing reaction was stopped by adding an equimolar amount of diethyleneglycol. The resulting

solution was dialyzed for 3 days against deionized water using a dialysis membrane with a MW cut off of 12000-13000 Da for CL-HA and for high MW HA or a dialysis membrane with a MW cut off of 1000 Da for low MW HA, and then lyophilized for 10 days using the freeze-dryer Scanlaf Scanvac 100-9 Pro Alpha 2-4.

3.1.3 – Preparation of oxidized hyaluronic acid-oxidized dextrin-ADH hydrogels

Hydrogels of oxidized Dex and oxidized HA were prepared as described in Molinos *et al.* [28] using different proportions: 100% Dex, 70% Dex - 30% HA, 50% Dex - 50% HA, 30% Dex - 70% HA, and 100% HA. Basically, oxidized HA and oxidized Dex were dissolved in PBS (30% w/v) buffer overnight at room temperature. Previously prepared ADH solution in PBS (3.76% w/v) was added to crosslink the solution in a 7:3 ratio (material:ADH). For the degradation assay, the solution was placed in a Teflon mould and allowed to gel and crosslink for 1h in a foam box with humid paper so the hydrogels would not dry during that time. For the other assays, the solution was allowed to gel in eppendorfs.

3.2 – Determination of the degree of oxidation by ^{1}H NMR Analysis

The DO of oxidized Dex and oxidized HA was quantified using ethylcarbazate (ETC) [41]. The samples - Dex, oxidized Dex, CL-HA, oxidized CL-HA - were dissolved in PBS to obtain a solution of 1% w/v each. In this preliminary assay, CL-HA was previously oxidized with a theoretical DO of 40%. ETC was added to the oxidized samples in a stoichiometric ratio of 5:1 (ETC:material). After dialysis for 3 days and lyophilisation of the material, the ^{1}H NMR spectra were recorded in D_2O and used to determine the DO. This is calculated as a peak area ratio in the NMR spectra according to Equation 3.1 where X is the average integral corresponding to the peak at δ 7.3 for Dex and for CL-HA and Y is the average integral of the anomeric protons at δ 5.4 for Dex or δ 2.0 for CL-HA.

$$\mathrm{DO}\ (\%) = \frac{\mathrm{X}}{\mathrm{Y}} \times 100 \qquad \textbf{(3.1)}$$

3.3 – Degradation Assay

After being prepared and weighted (W_i), 500µl hydrogels with different proportions and from different types of HA (CL-HA, high MW, and low MW) were immersed in PBS (pH 7.4) and incubated at 37ºC. For each condition, samples in triplicate were analyzed, except after day 5 using CL-HA where only one sample was used. At regular intervals, the hydrogels were removed from the solution, blotted with filter paper to remove the excess of PBS, weighted

(W_t) and returned to the same container. The buffer solution was replaced at each measurement and the percentage of mass loss can be determined by Equation 3.2.

$$\text{Mass loss } (\%) = 100 - \left(\frac{W_t}{W_i} \times 100\right) \qquad \textbf{(3.2)}$$

3.4 – Cell Culture and Seeding

MG-63 osteoblast-like cells, originally isolated from a human osteosarcoma [21], were used for this experiment. MG-63 cells have been well characterized and widely used for testing biomaterials. These cells were seeded in 100µl 50:50 Dex:CL-HA hydrogels and in 100% CL-HA hydrogels and maintained in α-MEM medium supplemented with 10% fetal bovine serum (FBS), 1% ascorbic acid, 1% Fungisoma and 1% Penicilin at 37ºC in the presence of 5% CO_2. Cells were seeded at a density of $5x10^4$ cells/well in the hydrogels after tripsinization at passage 10. Cl-HA and Dex were previously sterilized by ethylene oxide and rest for more than 20 days before use.

After analysing the obtained preliminary results, a second cell culture was performed using only 50:50 Dex:CL-HA (n=2), 100% CL-HA (n=2) and 100% Dex (n=3) hydrogels. The hydrogels were maintained in 37ºC at 5% CO_2 with complete α-MEM medium for 1h to remove any traces of non-linked ADH so that it would not acidify the medium and decrease cell viability. Since a change in colour was observed, the medium was removed and substituted with fresh one in the same conditions, for 30 minutes. After that time, the medium was removed and cells were seeded at a density of $3.5x10^4$ cells/well in the hydrogels (passage 11).

3.5 – Resazurin Viability Assay

Viablity was quantified by performing a resazurin assay one, two, five and seven days after seeding MG-63 cells in 50:50 Dex:CL-HA and 100% CL-HA hydrogels. Viability in 100% Dex hydrogels was also quantified by performing a resazurin assay 5h after seeding MG-63 cells. The medium was removed from the wells and 1ml of resazurin solution (10%) was added in the dark. The samples were incubated for 3h and then transferred to a 96-well plate to read the fluorescence in a Power Wave XS2 spectrophotometer (Biotek) at 530 nm excitation wavelength and 590 nm emission wavelength.

3.6 – MTT Assay

Viability was also analyzed by performing an MTT assay two days after seeding the cells in the hydrogels (50:50 Dex:CL-HA (n=2) and 100% CL-HA (n=2)). The medium was removed

from the wells and PBS was added to remove any dead cells and cell debris. MTT solution (10%) was added in each well and samples were incubated for 2h30 at 37ºC, 5% CO_2. The supernatant was discarded and 1ml of DMSO was added to dissolve the formazan crystals. 100µl of the supernatant was transferred to a 96-well plate to read the optical density at 550 nm in a Power Wave XS2 spectrophotometer (Biotek).

3.7 – Histocompatibility Assays

Oxidized CL-HA and oxidized Dex were previously sterilized by ethylene oxide and rest for 10 days before use. 100µl hydrogels were surgically implanted subcutaneously in the lumbar region of three male rats (Sasco Sprague Dawley, Barcelona, Spain, weighting around 300 g), each one receiving three implants of 50:50 Dex:CL-HA hydrogels and two of 100% CL-HA hydrogels. Previous experimental work already evaluated the biological response of the rats using 100% Dex hydrogels as well as a control with no implant but where the suture was performed (Sham group). Two animals were housed per cage (Makrolon type 4, Tecniplast, VA, Italy), in a temperature and humidity controlled room with 12-12h light/dark cycles, and were allowed normal cage activities under standard laboratory conditions. The animals were fed with standard chow and water *ad libitum*. Adequate measures were taken to minimize pain and discomfort taking into account human endpoints for animal suffering and distress. All procedures were performed with the approval of the Veterinarian Authorities of Portugal, and in accordance with the European Communities Council Directive of November 24th 1986 (86/609/EEC). Anaesthesia was achieved with an intraperitoneal injection of a pre-mixed solution consisting in ketamine (Imalgène 1000®), 100 mg/kg body weight, and xylazyne (Rompun®), 200 mg/kg body weight. Hair from the dorsal area was clipped and the skin scrubbed in a routine fashion with an iodopovodone 10% solution (Betadine®). Five 1.5-2cm long linear incisions were performed. After blunt dissection towards the ventral aspect of the body, the two types of biomaterial were implanted subcutaneously. Skin and subcutaneous tissues were closed with a simple-interrupted suture of a non-absorbable filament (Synthofil®, Ethicon). The macroscopic aspect of the wound and the absence of inflammation and/or infection were clinically checked by a veterinary before the surgical extraction of the implants and surrounding tissues. On days 3, 7 and 14, one animal was randomly selected; after performing the same anaesthetic protocol, skin and subcutaneous tissues from the implant area were collected and fixed in a container with 10% neutral buffered formalin (Panreac, Portugal) for posterior histological evaluation using ISO score as previously described. The rats were then euthanized, by lethal intracardiac injection of 5% sodium pentobarbital (Euthasil®). Samples were routinely processed, and 5 µm-thin sequential sections were stained with hematoxilin-eosin (HE). Slides were examined under a light microscope (Nikon E600), and photographs were obtained using a digital camera (Nikon DS-5M).

Chapter 4

Results and Discussion

4.1 – Production of hyaluronic acid and dextrin hydrogels

4.1.1 – Preparation of the material

Lyophilisation of oxidized Dex and oxidized HA had an efficiency of 89.8% and 89.3%, respectively. Dex, CL-HA and high MW HA appeared white and fluffy after oxidation and lyophilisation. However, due to a problem during the lyophilisation of low MW HA, it started to hydrate after a few days which means a second lyophilisation of this material was necessary. This resulted in a brittle and fragile material. In addition, it appeared a little more yellow than CL-HA and high MW HA.

4.1.2 – Different testing conditions

There are several parameters to be considered when designing hydrogels including concentration and source, nature of the crosslinking agent, proportion of the crosslinking agent versus polymer, among others.

HA fragments have highly wide-ranging and often opposing biological functions. Large HA polymers are space-filing, anti-angiogenic, immunosuppressive, and prevent differentiation maybe due to the suppression of cell-cell interactions or ligand access to cell surface receptors. However, smaller HA fragments are inflammatory, immune-stimulatory and angiogenic, and compete with large HA polymers for receptors [42]. Various fragments trigger different signal transduction pathways. High MW HA can function as a lubrificant, shock absorber and as a space-occupying material as in WJ where it may suppress compression of the umbilical cord. This type of HA is highly involved in the processes of ovulation, fertilization and embryogenesis, also inhibiting phagocytosis by monocytes and macrophages.

In addition, high MW HA promotes cell cycle arrest, protects cells against injury and maintains epithelial cell integrity. [42] CL-HA consists in a network of HA chains which have been covalently linked by chemical processing which results in macroscopic HA hydrogel materials with viscoelastic properties that are not characteristic of HA hydrogel solutions [43]. This way, in order to check the effect of HA with different size, the following kinds of HA were tested: CL-HA, high MW HA and low MW HA.

As explained before, HA may have the ability to delay the differentiation of MSCs. However, functionalization of the material regarding degradation rate is also important for future applications so different proportions of Dex and HA were used to analyse the different properties of the resulting hydrogels. Dex hydrogels have fast degradation, with 100% mass loss in 24h *in vitro*. However, for the here defined goal, the hydrogel should last a few days before complete degradation so different proportions of Dex and HA were tested to help choosing the hydrogel with lowest degradation rate.

Due to the different properties of the resulting hydrogels, they appear with different colours. Regarding the hydrogels produced with low MW HA, they become orange coloured with the increase of HA percentage, as it can be seen in Figure 4.1, maybe due to the second lyophilisation step. However, there is no major difference in colour between the hydrogels produced with high MW HA (Figure 4.2) or CL-HA (Figure 4.3) with different ratios, and they appeared transparent, similar in colour to hydrogels without HA (Figure 4.3).

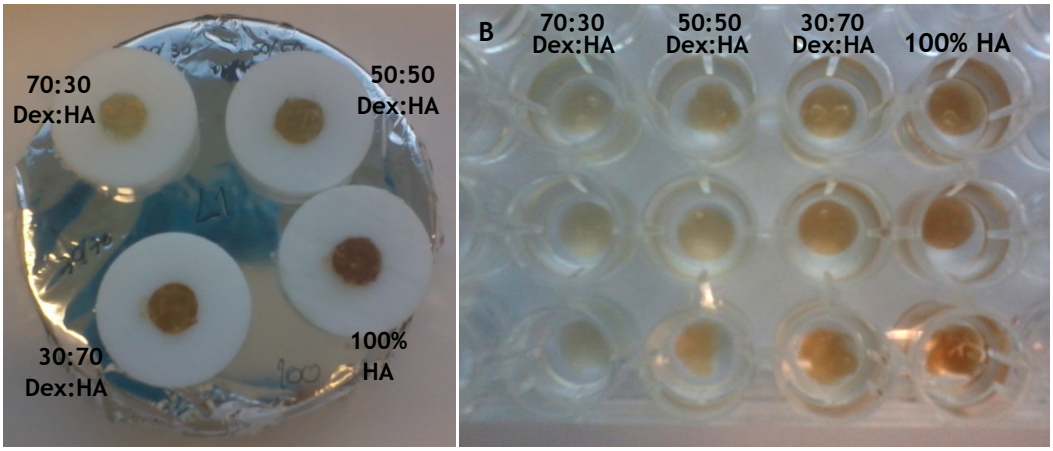

Figure 4.1. Dex and low MW HA hydrogels with different proportions in the moulds (A) and in a PBS solution (B).

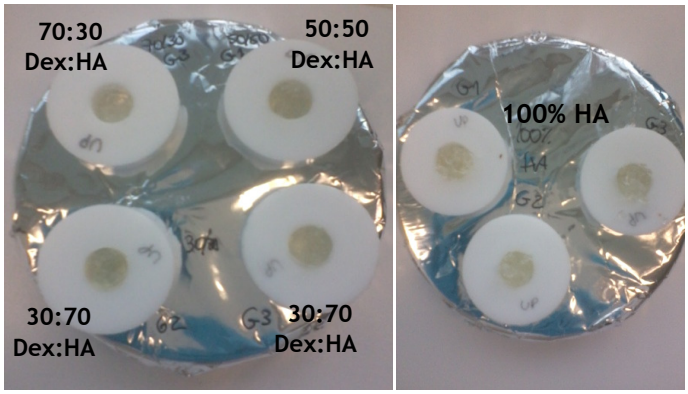

Figure 4.2. Dex and high MW HA hydrogels with different proportions in the moulds.

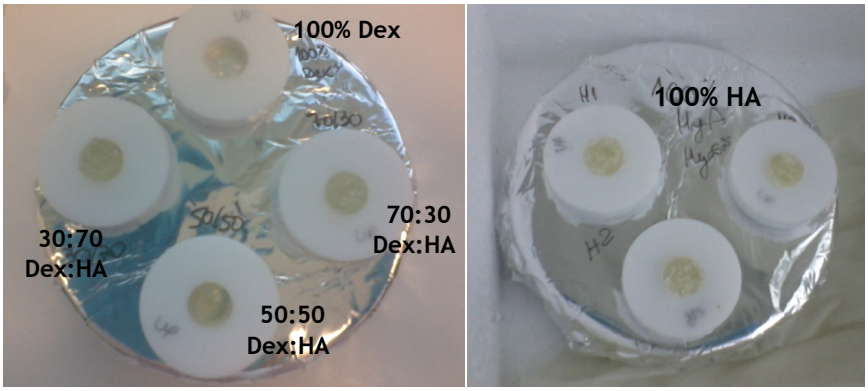

Figure 4.3. Dex and CL-HA hydrogels with different proportions in the moulds.

4.1.3 – Gelation time

The gelation time of the hydrogels can be seen in Table 4.1. Dex and HA were dissolved in eppendorfs before adding the crosslinker ADH. Since high MW HA and CL-HA are highly hygroscopic and have viscous properties [44], their solubility is lower than that of low MW HA which resulted in hydrogels (or highly viscous solutions) of Dex and HA still inside the eppendorfs before the addition of ADH. In other hand, due to the high solubility of low MW HA, the material Dex plus low MW HA was still liquid. Despite becoming a gel without the crosslinker, ADH was still added to each solution in the referred proportions and the material was transferred to Teflon moulds. According to Aurande *et al.* [29] and Figure 2.11, hydrogels with more than 1% HA polymerize very quickly, within less than 30 seconds. Our results agree with this finding.

In addition, a lower gelation time was observed with an increase in the percentage of HA. Since HA is rather viscous, the solution polymerizes very quickly. However, since low MW HA is similar to Dex in MW, the solution is not as viscous as the others and the polymerization time increases.

Table 4.1. Gelation times for Dex and HA hydrogels according to each proportion and type of HA.

Type of HA	Gelation time of Dex and HA hydrogels			
	70:30 Dex:HA	50:50 Dex:HA	30:70 Dex:HA	100% HA
Low MW HA	1min	1min	< 1min	< 1min
High MW HA	< 1min *	< 1min *	< 1min *	< 1min *
CL-HA	< 1min *	< 1min *	< 1min *	< 1min *

*The material polymerized in the eppendorfs before the addition of ADH.

Regarding 100% Dex hydrogels, gelation occurred in 4 min which can be explained by the fact that Dex has high solubility and is much less viscous than HA. According to Molinos *et al.* [28] and Table 2.1, since the theoretical DO of the 100% Dex hydrogel is 40% and ADH has a concentration of 3.76% w/v, the obtained value for gelation period should be more than

2min. This way, the gelation period obtained for the 100% Dex hydrogel agrees with the literature.

During crosslinking, oxidized HA (Figure 4.4.A) and oxidized Dex (Figure 4.4.B) react with ADH (Figure 4.4.C), resulting in the formation of Dex and HA hydrogels, and of its copolymers.

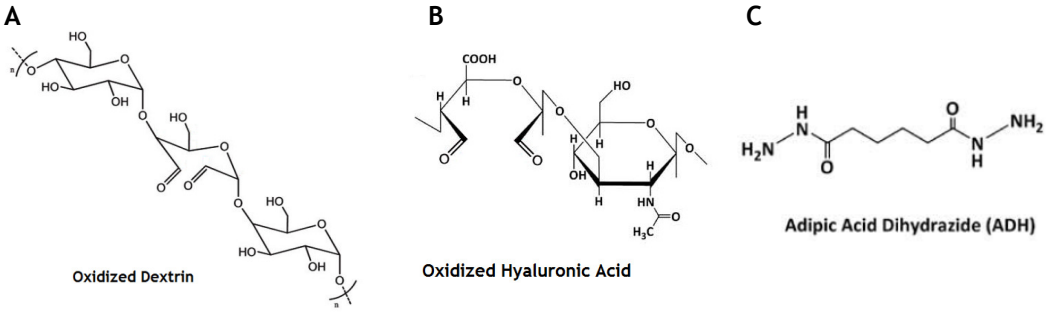

Figure 4.4. Basic chemical structure of oxidized Dex (A), oxidized HA (B) and ADH (C).

4.2 – Determination of the degree of oxidation by ^{1}H NMR Analysis

Determination of aldehyde groups allows the quantification of the DO of Dex and CL-HA. In this assay, the carbazates react with aldehyde groups to form carbazones [45]. The chemical shifts are represented in parts per million (ppm). The analysis of Dex and CL-HA will be performed based on Figures 4.5 and 4.6, respectively, and Table 4.2 and 4.3.

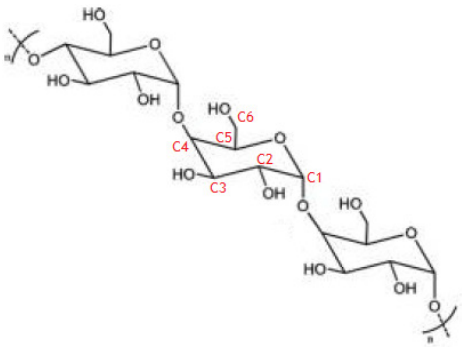

Figure 4.5. Chemical structure of Dex with notation in which ^{1}H NMR analysis is based.

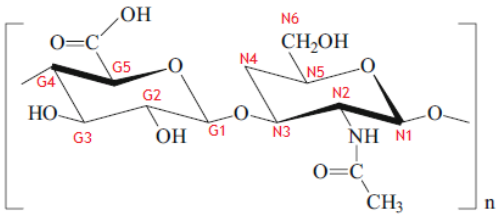

Figure 4.6. Chemical structure of HA with notation in which ^{1}H NMR analysis is based.

Table 4.2. Chemical shift and its structural correspondence for ^{1}H NMR for Dex [28].

Chemical shift (ppm)	Structural correspondence
δ = 3.4 - 4.0	C2, C3, C4, C5, C6
δ = 5.4	Glucose anomeric proton corresponding to α-1,6 linkage
δ = 7.2 - 7.4	Proton attached to the carbon with linked ETC

Table 4.3. Chemical shift and its structural correspondence for ^{1}H NMR for HA [46].

Chemical shift (ppm)	Structural correspondence	Chemical shift (ppm)	Structural correspondence
δ = 4.51	G1	δ = 3.92	N2
δ = 3.40	G2	δ = 3.74 – 3.85	N3, N6, G4, G5
δ = 3.63	G3	δ = 3.51 – 3.62	N4, N5
δ = 4.61	N1	δ = 2.07	$NCOCH_3$

In homopolysaccharides such as Dex and HA, the oxidation reaction is characterized by the opening of the glucopyranoside rings between C2 and C3 (in Dex) and in G2 and G3 (in HA). DO can be easily controlled by the relative quantity of sodium periodate used, yielding free aldehyde reactive groups to create covalent linkages with crosslinking agents, cellular adhesion binding peptides or specific drugs for targeted controlled delivery systems [28]. Due to the highly reactive nature of the formed aldehydes, they are easily attacked by neighbouring hydroxyl groups, leading to the formation of hemiacetals. In Dex, only one aldehyde per residue might be involved in Dex oxidation, while the second aldehyde can be arrested to a stable hemiacetal structure [47].

Using Equation 3.1 and the data from Figure 4.7, the experimental DO for oxidized Dex is 29%, which is, as expected, lower than the theoretical value of 40%. The oxidation reaction in Dex has an efficiency of about 74%, in agreement with the literature [48]. This indicates that 29 in 100 disaccharides of Dex have one ring open for future crosslinking.

By comparing Figure S.3 and S.4 it is possible to see that around the chemical shift of 2 ppm a peak from CL-HA resulted in two peaks in oxidized CL-HA. This indicates that there was a change in the conformation caused by the opening of one of the rings and the gain of electrons in G2 and G3. The analysis of Figure 4.8 suggests that CL-HA has a DO below 40%, since the peak at 7.3 ppm (which corresponds to the proton attached to the carbon with linked ETC) is very small. This does not allow an effective calculation of the DO. Since CL-HA has a very low solubility, quantifications of the aldehyde groups become very difficult. In previous studies [31] low MW HA was oxidized under conditions corresponding to a theoretical value of 100%. The experimental value obtained was 44% [31]. According to this oxidation

efficiency, the expected value in the present situation should be around 18%. However, it is not possible to infer about the oxidation efficiency in these conditions. In the following assays, HA was oxidized with a theoretical DO of 100%.

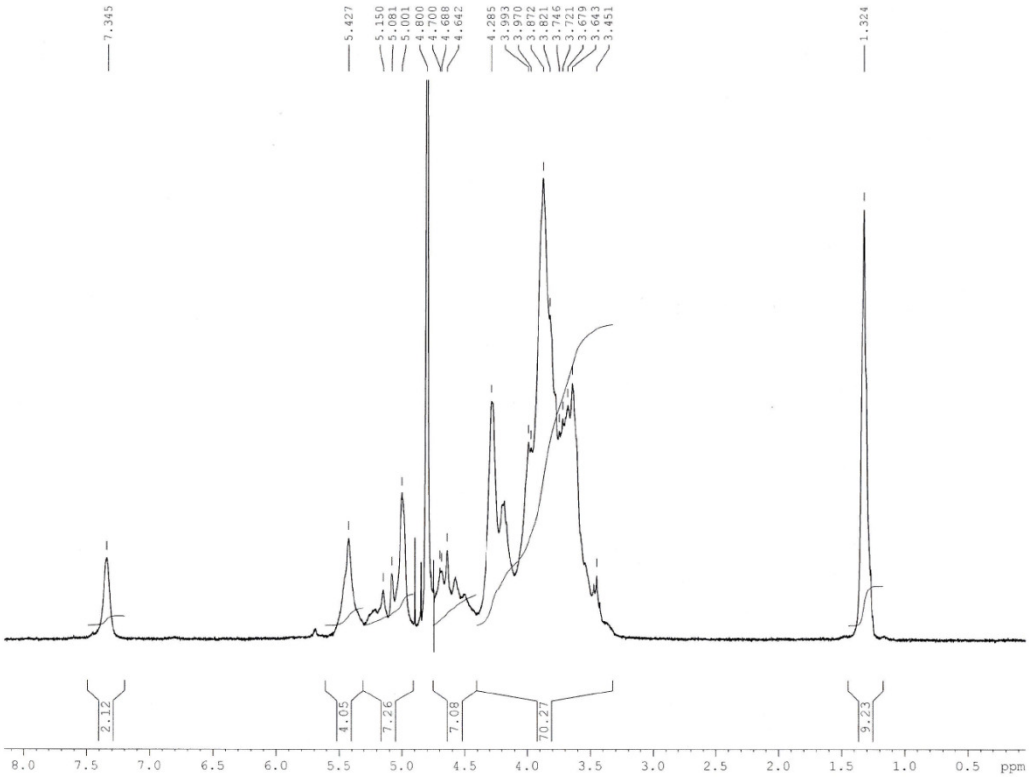

Figure 4.7. ^{1}H NMR spectrum of oxidized Dex with ETC.

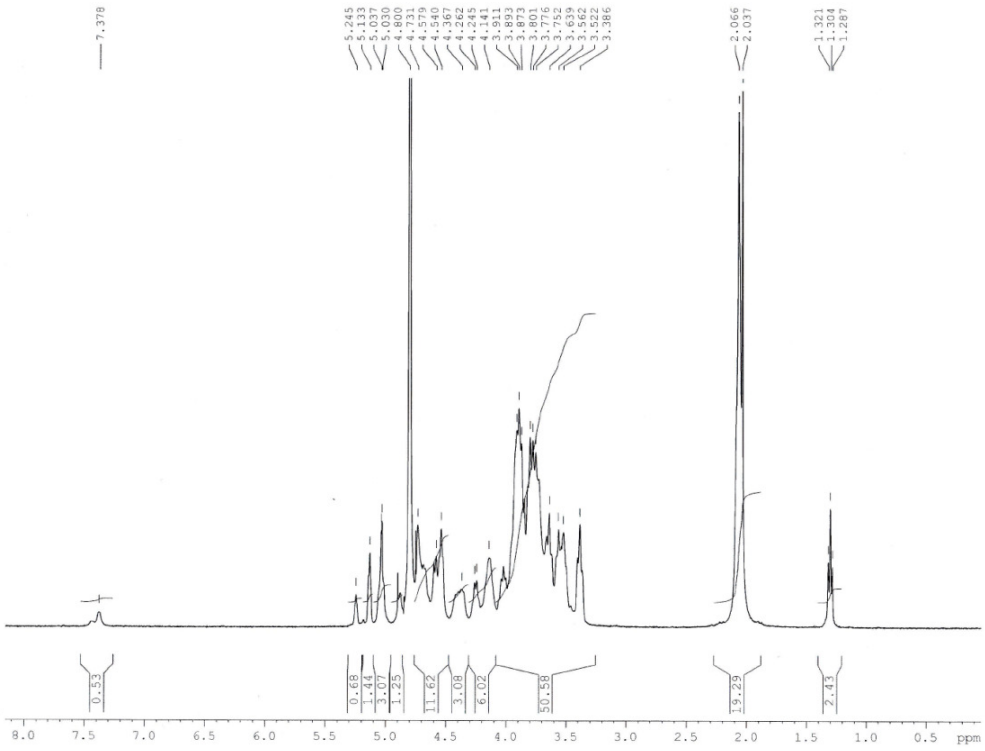

Figure 4.8. ^{1}H NMR spectrum of oxidized CL-HA with ETC.

4.3 – Degradation Assay

The degradation rate of the resulting hydrogels was analysed to help choosing the better ratio of the copolymers. 500 µl hydrogels were produced using different combinations of HA-Dex. Hydrogel degradation depends on the chemical structure of the polymer backbone and can occur by surface or bulk erosion. Surface erosion occurs when the rate of erosion exceeds the rate of water permeation into the bulk of the polymer. On the other hand, bulk erosion occurs when water molecules permeate into the bulk of the matrix at a faster rate than erosion, exhibiting complex degradation and erosion kinetics. In hydrogels produced from biodegradable polymers such as Dex and HA, degradation occurs mainly by bulk erosion and it is characterized by nonlinear degradation profile and an increasing pore size [28].

By observing Figures 4.9 to 4.11, it is possible to see that hydrogels produced with low MW HA degrades faster than the others. In this case, low MW HA and Dex mixture seems to not to led to a mutual interaction, with a fast degradation being observed. There is no clear trend regarding the effect of varying the ratio between the two polymers. Kim *et al.* [44] reported that 10 wt % hydrogels with 10 kDa acrylated HA degraded slowly by hydrolysis, with 40% mass loss after 45 days, which does not agree with the obtained results. One may speculate that the second lyophilisation performed with the low MW HA may have had some impact in the observed behaviour. The fast degradation may be due to both polymers having high solubility, hence higher water affinity, resulting in faster bulk degradation.

In some of the hydrogels used in this assay (100% Dex, 70:30 Dex:low MW HA, 100% low MW HA, 100% high MW HA, 70:30 Dex:CL-HA and 100% CL-HA), the initial phase of the mass loss curve bears increased weight, which represents the occurrence of swelling. This is very important for cell survival since nutrients must be able to penetrate into the hydrogel. This way, their ability to absorb water is highly important [49][50]. Since Dex and HA are hydrophilic, it would be expected to see the initial swelling phase for 100% Dex and 100% HA hydrogels, an effect also related to osmotic pressure. Since 100% Dex hydrogels have a higher swelling, one may hypothesize that Dex is a) more hydrophilic than HA, b) the Dex hydrogel is more porous or, c) it presents higher osmotic forces (this is quite likely, since Dex has a much lower MW than HA), explaining the higher degradation rate. During degradation, initially a small number of crosslinked bonds are broken which do not compromise the whole hydrogel network but instead increases its lattice size, resulting in a large water absorbance and further hydrolysis. This results in a faster degradation, as seen in the referred hydrogels. After the broken crosslinked bonds reached a critical value, the crosslinking network dissociates and mass loss is observed.

Analysing Figures 4.9 to 4.11 it is possible to conclude that the weight loss increases with the Dex contents, suggesting that the degradation is depending on the dissociation/dissolution of Dex from the hydrogels. Since Dex and HA have a high water-binding capacity, they should be dissolved quickly in water as the hydrazone bonds undergo

hydrolysis. Further trials must be performed to confirm the observed trend of a lower degradation of the 100% HA hydrogel, followed by a rather fast degradation. The mixed hydrogels apparently bear a steady rate of mass loss. Su *et al.* [31] reported that 6%wt oxidized HA (with a MW of 320 kDa) hydrogels crosslinked with 4% ADH degraded after 12 days. The obtained results for 100% high MW HA and 100% CL-HA hydrogels agree with these results despite the difference in MW and polymer concentration. In the same report [31], hydrogels in the same conditions but crosslinked with 2% ADH degraded in three days which implies that a lower concentration of the crosslink agent increases the degradation rate. Due to the high viscosity of the material, its crosslinking is difficult and influences the degradation rate.

In each hydrogel, the degradation rate slows down after a few days since the cleavage of hydrazone bonds by water has reached a critical value. It is also possible to see that hydrogels produced with high MW HA or CL-HA have a better degradation rate. In this situation, the proportions with the lowest degradation rate are 50:50 and 30:70 Dex:HA which suggests that the interaction between Dex and HA delay degradation maybe due to the three dimensional lattice that retains the degraded material inside. Throughout degradation, it is possible to see that hydrogels with high MW HA or CL-HA change colour from transparent to orange which implies that HA chains are being released since hydrogels appear with the same colour as low MW hydrogels.

It is possible to conclude that the degradation rate can be tuned and controlled by altering the material proportions or/and its concentration.

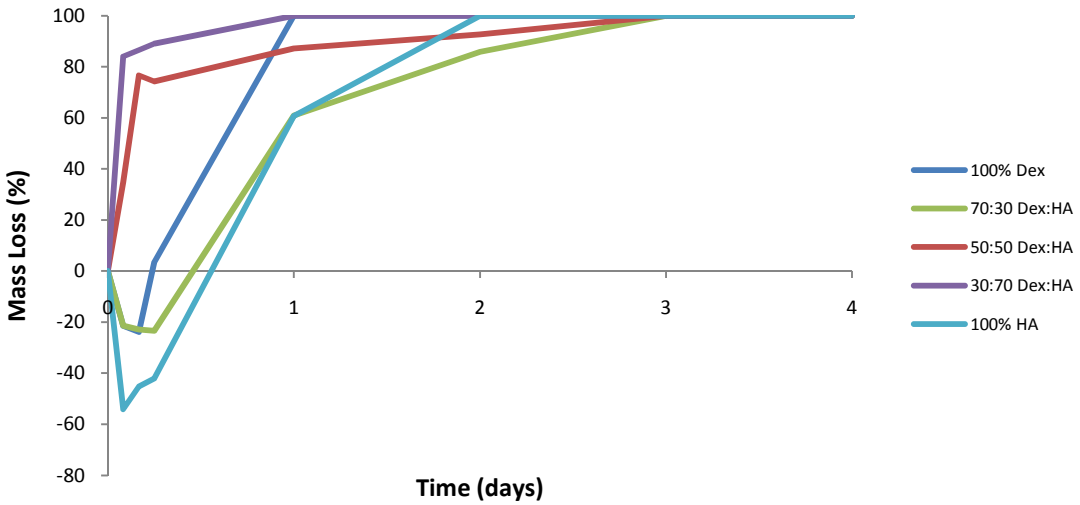

Figure 4.9. Degradation profile of Dex and low MW HA hydrogels (n=3) in PBS.

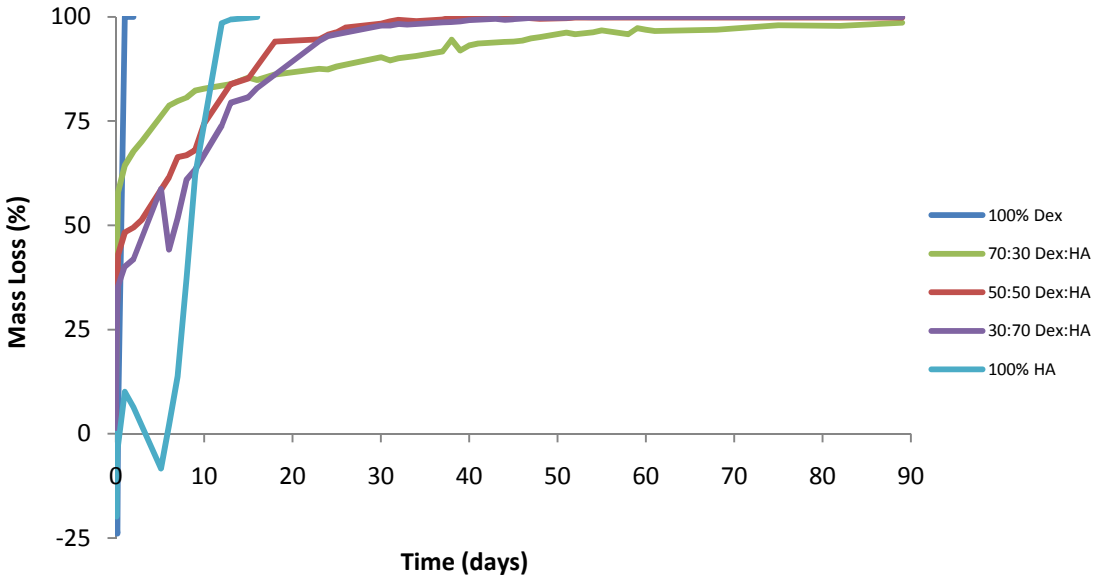

Figure 4.10. Degradation profile of Dex and high MW HA hydrogels (n=3) in PBS.

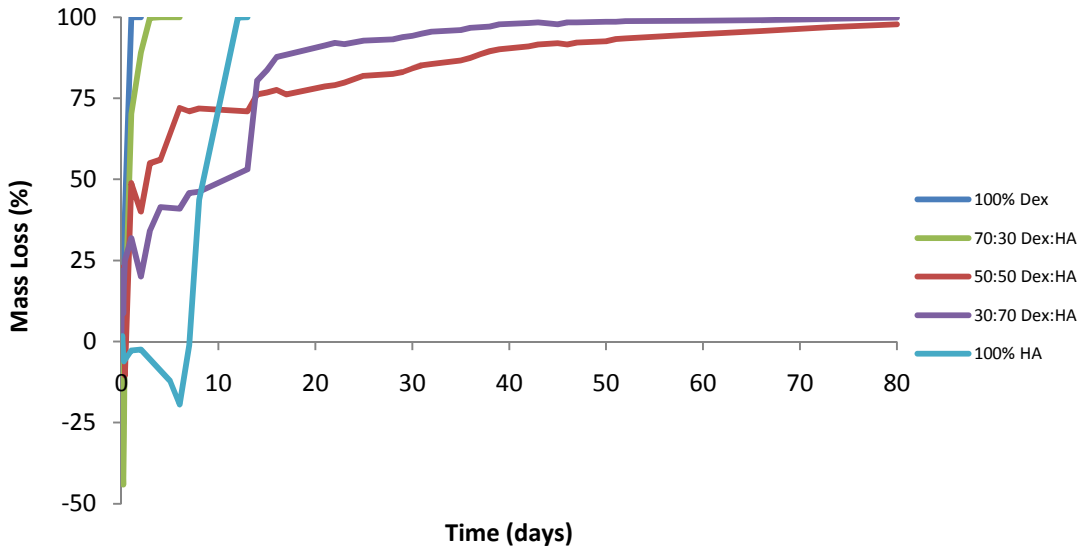

Figure 4.11. Degradation profile of Dex and CL-HA hydrogels (n=3 until day 5, n=1 after day 5) in PBS.

4.4 - Resazurin Viability Assay

A resazurin assay was performed to evaluate cellular viability in the hydrogels. Due to the lack of material only 50:50 Dex:HA and 100% HA hydrogels were used in this assay. One day after seeding, it was observed that the medium with hydrogels became orange, comparing with the pink control medium (Figure 4.12). This indicates that the medium was turning acid, which is likely due to non-linked ADH. The pH observed (7.0) is normally not dangerous enough for the cells, which optimally require pH 7.4. This loss of viability *in vitro* in absorbable materials is quite frequent due to the change of pH. However, when working in

closed systems, as the *in vitro* assays performed in this work, the dilution effects does not occur whereas the constant change of fluids *in vivo*, prevent the accumulation of degradation products at high concentrations [29]. A classic example of this fact is gluteraldehyde, which is a widely used cross-linker, often considered cytotoxic *in vitro*, even at low concentrations [52][53]. However, it is still used for reticulation of biomedical products [54]. A resazurin assay was still performed for days 1, 2 and 5 after seeding (Figure 4.13) and microphotographs were taken (Figure 4.14).

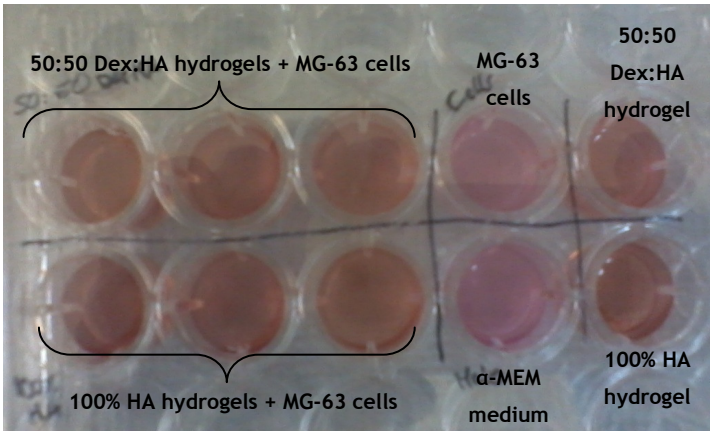

Figure 4.12. Macroscopic analysis of the hydrogels and MG-63 cells one day after seeding.

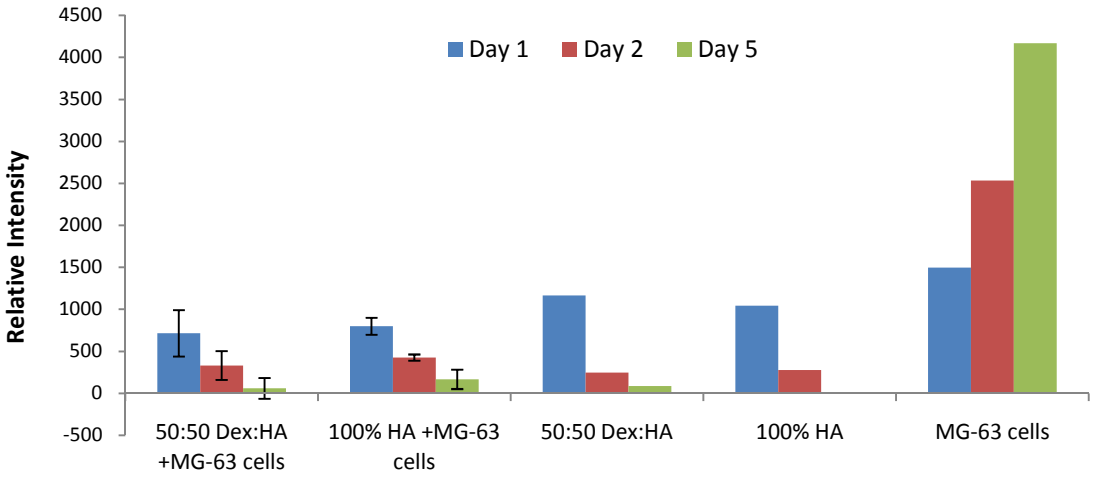

Figure 4.13. Relative intensity of the hydrogels with MG-63 cells (n=3), hydrogels without MG-63 cells (n=1) and the cellular control (n=1) using fluorescence at 530 nm excitation wavelength and 590 nm emission wavelength.

Probably due to the acid medium previously explained, MG-63 cells in the hydrogels started to die and bear a round shaped morphology, as seen in Figure 4.14. However, since there was no influence of the hydrogel in the cellular control, MG-63 cells presented increased viability with time. In addition, samples with only hydrogels and without cells also appeared with high viability for day 1 which may suggest that Dex and HA interfere with resazurin, occurring false positive results.

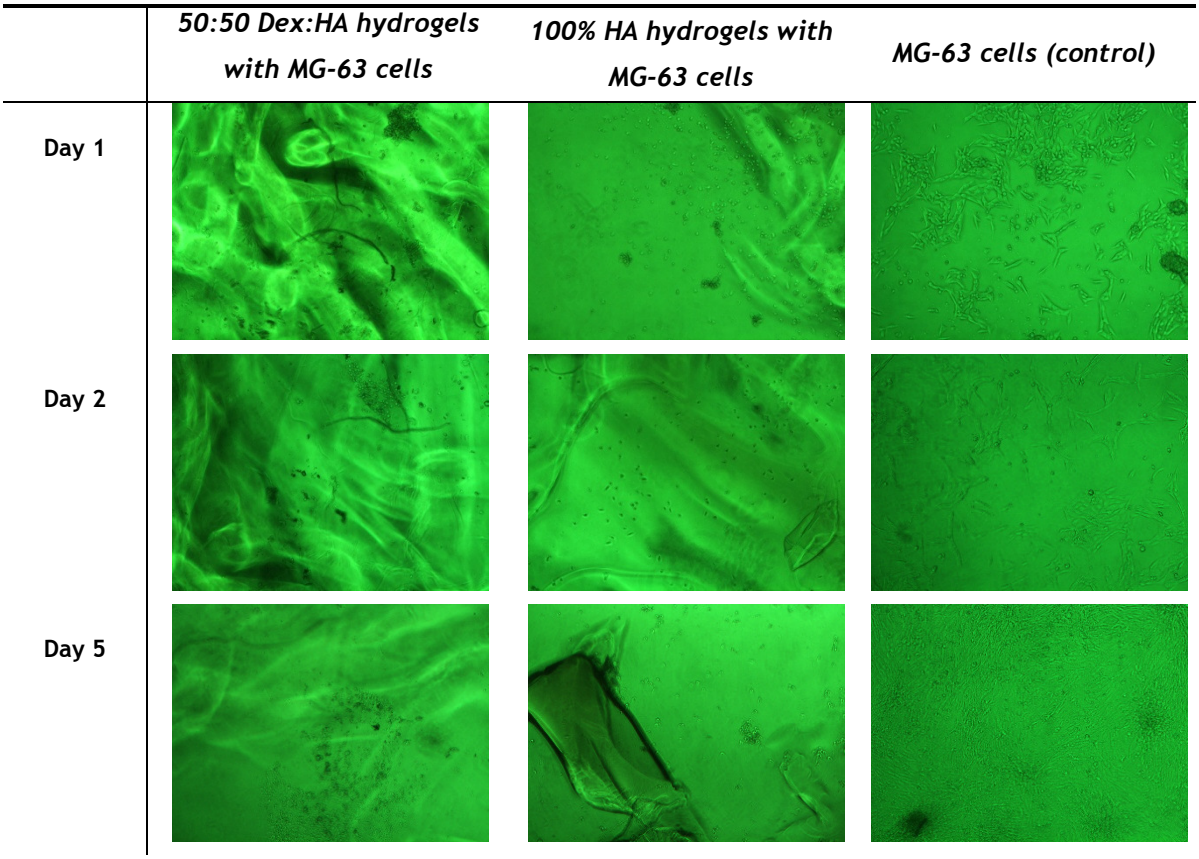

Figure 4.14. Microscopic analysis of the hydrogels and cells one, two and five days after seeding (amplification: 40x).

A second cell culture was performed with a different method. Before cell seeding, the hydrogels were maintained in α-MEM medium until there was no change in colour. This step was included to remove non-linked ADH that could damage the cells. This resazurin assay was performed for days 1, 2, 5 and 7 after seeding. Figures 4.15 and 4.16 show that metabolically active MG-63 cells were present in 100% HA hydrogels and in the cellular control. In these hydrogels cells appeared elongated, with increasing viability over time. However in 50:50 Dex:HA hydrogels the number of metabolically active MG-63 cells was very low and cells presented a round shaped morphology. In a previous work (data not shown) cell viability in Dex hydrogels through a live and dead assay were assessed. In this study, mouse embryo 3T3 fibroblasts were encapsulated in oxidized Dex hydrogels and live and dead fluorescence was analysed after 6h of incubation, the exactly time point when the hydrogel when the mass loss begins. Results indicated that the majority of the cells that were kept encapsulated in the dex hydrogel (98.2±1.9%) were calcein positive (viable) cells and that cells could endure the cross-linking stage, thus becoming a suitable platform for the incorporation of cells to be used for tissue engineering purposes. Another explanation for this behaviour was due to the fact the hyaluronic acid is a much more viscous material, even in solution, a fact that difficults the homogenization of the solutions of Dex/HA with ADH. A poorly mixture of these components will probably cause a great amount of non-linked aldehyde groups, which can result in a higher degree of cytotoxicity. In addition, non-linked ADH could be present inside

the hydrogel and being released throughout time due to degradation. Figure 4.18 also shows that the viability assay using resazurin presents high intensity in the samples without cells, which can indicate false positive results.

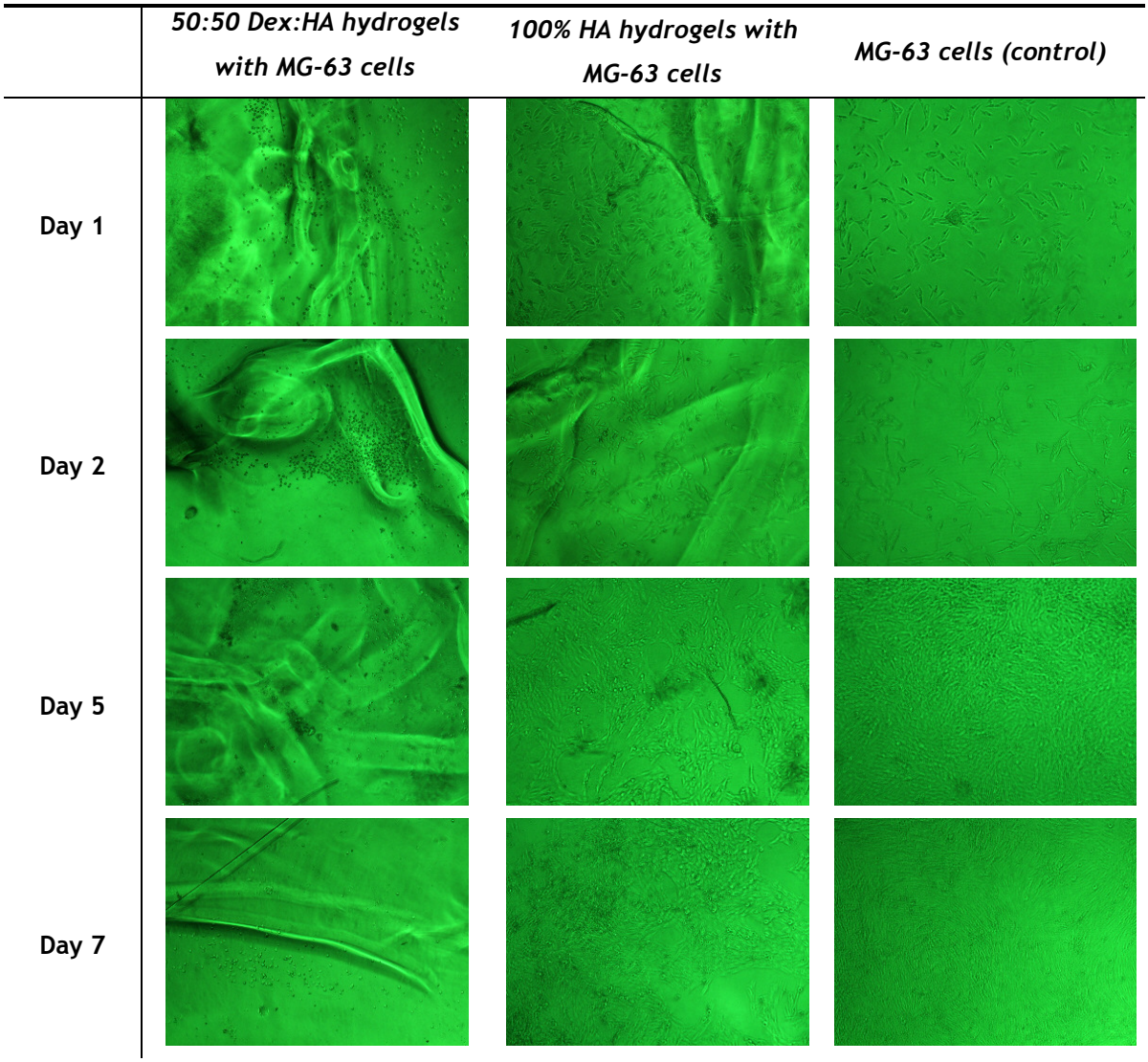

Figure 4.15. Microscopic analysis of the hydrogels and cells one, two, five and seven days after seeding and treatment of the hydrogels (amplification: 40x).

A viability assay using resazurin was also performed in 100% Dex hydrogels. Since these hydrogels have a high degradation rate, viability was measured 5h after their production. Results (Figure 4.17) suggested that MG-63 cells have higher viability in the hydrogels than in the control. These results are consistent with previous works showing high viability obtained by live and dead assays and also with the subcutaneous implants performed with Dex hydrogels incorporating human mesenchymal steam cells. Histological analysis of these assays revealed the presence of these cells in the soft tissue surrounding the implant site. Few hours may not be enough for cell adhesion to occur. Due to the processes involved in this measurement, there could be a decrease in cells numbers when the α-MEM medium was removed and substituted by the resazurin solution. This way, this test may reveal more about

cell adhesion than viability, indicating a higher cell adhesion in the hydrogels than in the control. A 3D matrix mimics better the microenvironment than 2D models. Chen *et al*. [51] analysed the effect of 3D and 2D cell cultures using osteosarcoma cells and observed that 3D fibrous culture had better cell growth and higher metabolic rates than 2D cultures since in a 3D environment cells are protected from shear stress. In addition, Chang *et al*. [55] studied the behaviour of MSCs in a 3D matrix and results showed better adhesion and growth rate in the 3D matrix than in the 2D culture. In a 3D matrix MSCs showed colocalization of α5 integrin and αv integrin which increased cell adhesion due to focal adhesions. [55] This may explain the higher values obtained for the cells in the hydrogel than in the control. Due to a malfunction in the equipment, it was not possible to obtain microphotographs of the cells.

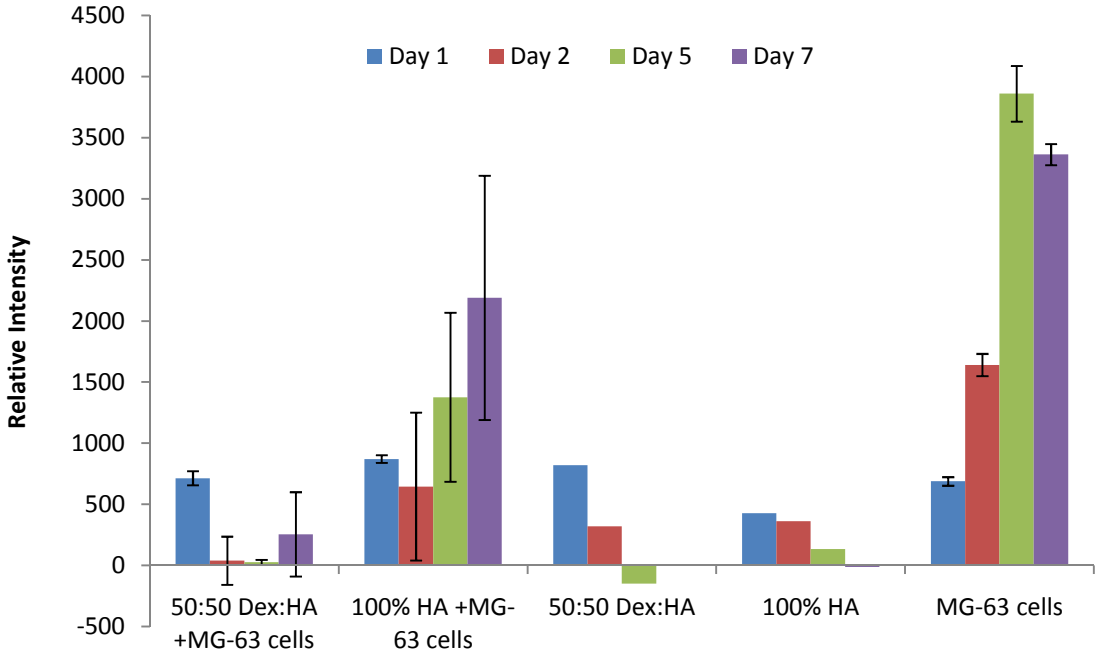

Figure 4.16. Relative intensity of the hydrogels with MG-63 cells (n=2), hydrogels without MG-63 cells (n=1) and the cellular control (n=2) one, two, five and seven days after seeding and treatment of the hydrogels using fluorescence at 530 nm excitation wavelength and 590 nm emission wavelength.

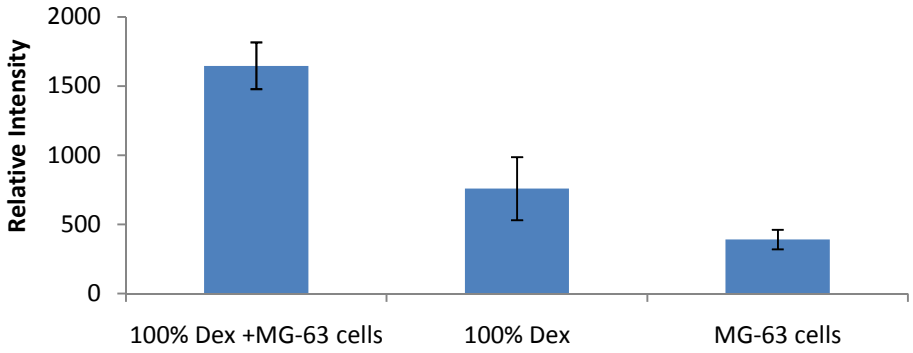

Figure 4.17. Relative intensity of the hydrogels with MG-63 cells (n=3), hydrogels without the MG-63 cells (n=2) and the cellular control (n=2) using fluorescence at 530 nm excitation wavelength and 590 nm emission wavelength 5h after the production of 100% Dex hydrogels.

4.5 – MTT Assay

Metabolically active and viable cells produce mitochondrial dehydrogenase enzymes during incubation in media, which is usually catalyzed by MTT salt. This reaction produces purple colored formazan which allows for the quantification of cell viability by measuring the change in colour intensity using a spectrophometer. An initial analysis was performed using an MTT assay after 2 days of incubation and results can be seen in Figures 4.18 and 4.19. In metabolically active cells, star-shaped morphology is observed due to the MTT colouring. Results indicate that, although the majority of the cells in the hydrogels appear dying and bear a round shaped morphology, the absorbance values indicate higher cell viability in the hydrogels with the cells than in the control of only MG-63 cells. This data does not agree with the results obtained from the resazurin assay (Figure 4.14) and from the visual analysis of Figure 4.18. Although some metabolically active cells with star-shaped morphology are present in the samples, it is not sufficient to result in higher values of absorbance than those from control. Moreover, samples with no cells implanted (50:50 Dex:HA and 100% HA hydrogels) also appeared with high values of absorbance which suggest that false positive results occur in the MTT assay and that Dex and HA interfere with MTT.

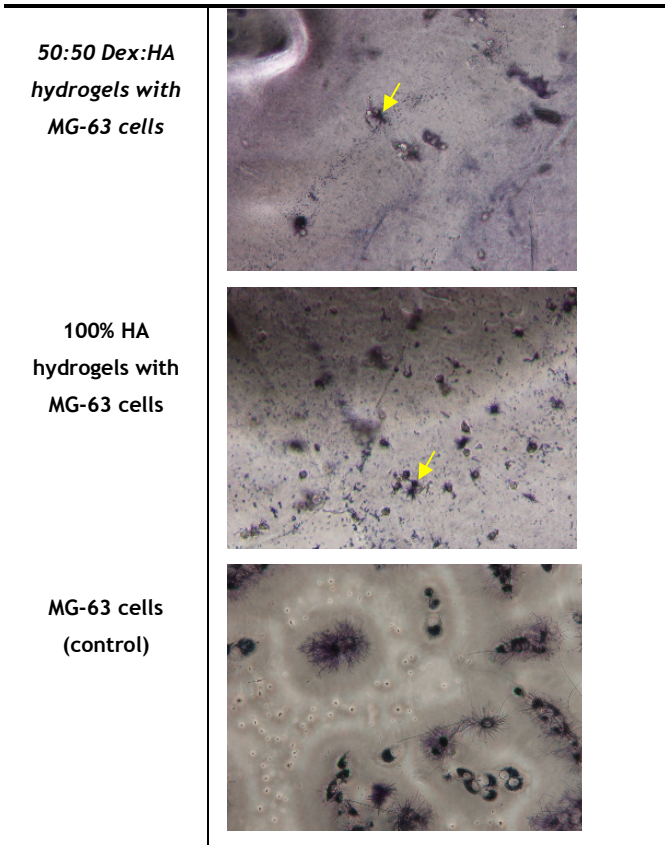

Figure 4.18. Microscopic photographs of the different hydrogels and the cellular control before the addition of DMSO to dissolve MTT. It is possible to observe metabolically active cells in the hydrogels (arrow) and in the control (amplification: 40x).

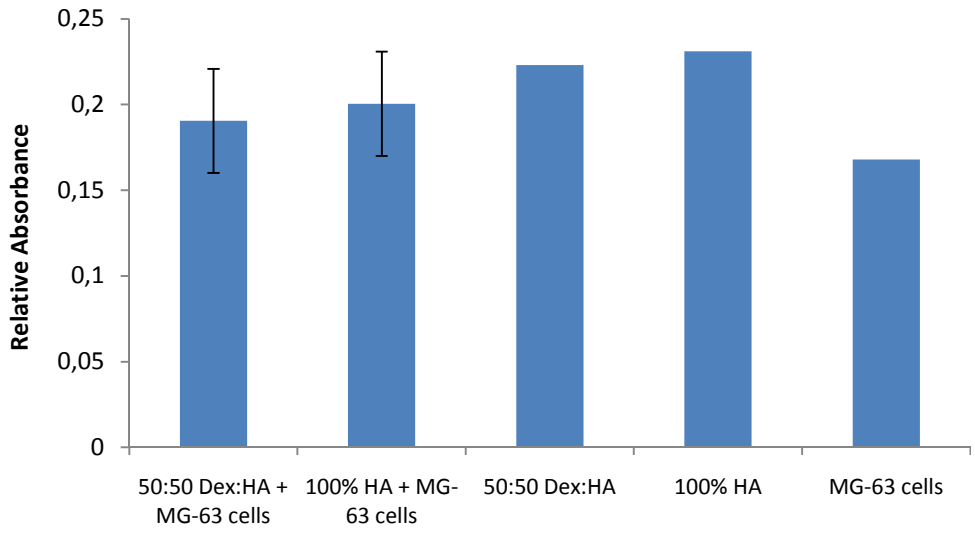

Figure 4.19. Relative absorbance for the hydrogels with MG-63 cells (n=3), hydrogels without MG-63 cells (n=1) and the cellular control (n=1).

4.6 – Histocompatibility Assays

A biocompatibility analysis should be performed to verify if a material can be used *in vivo*. The FDA relies on ISO 10993 Standard to test biocompatibility and cytotoxicity of a material and the analysis can be performed using histological samples of the tissues where the biomaterial was implanted. Due to the low gelation time, it is not possible to inject the material in *in vivo* applications so the hydrogels must be produced in eppendorfs and then placed subcutaneously in the lumbar region of rats. Evaluation was performed at 3, 7 and 14 days after implantation for 50:50 Dex:CL-HA (n=3) and 100% CL-HA (n=2) hydrogels. Data from previous reports using 100% Dex hydrogels was used. Figure 4.20 shows the macroscopic analysis of the necropsy of the mice where the hydrogels were implanted. No macroscopic signs of inflammation, cytotoxicity or fibrosis were found.

When a material is implanted in the body, several processes occur including injury, blood-material interactions, provisional matrix formation, acute inflammation, chronic inflammation, granulation tissue development, foreign body reaction, and fibrosis or fibrous capsule development [56]. The extent or degree of the inflammatory reactions is controlled by the extent of injury in the implantation procedure, the tissue into which the biomaterial is implanted, and the extent of the provisional matrix formation. Each stage is characterized by different cell types, as seen in Figure 4.21. Acute inflammatory response is characterized by neutrophils (polymorphonuclear leukocytes) and is mediated by mast cell degranulation with histamine release and fibrinogen adsorption. On the other hand, chronic inflammation is identified by the presence of mononuclear cells, such as monocytes, lymphocytes and plasma cells, at the implant site [57]. Chronic inflammation has been also used to describe the foreign body reaction where monocytes, macrophages, and foreign body giant cells are

present at the biomaterial interface. The persistence of inflammatory responses beyond a three-week period usually indicates an infection. Using biocompatible materials, chronic inflammatory response usually lasts no longer than two weeks. Following resolution of these phenomena, the formation of granulation tissue is identified by the presence of macrophages, the infiltration of fibroblasts, and neovascularisation in the new healing tissue. In the foreign body reaction, there is a release of cytokines that stimulate inflammation and fibrosis. This response is characterized by multinucleated giant cells that result from fusion of macrophages [56].

Hydrogels have advantages in biocompatibility. Their swelling capacity allows the expulsion of impurities, decreasing the inflammatory responses. In addition, hydrogels decrease the frictional and mechanical irritation of the tissues [58].

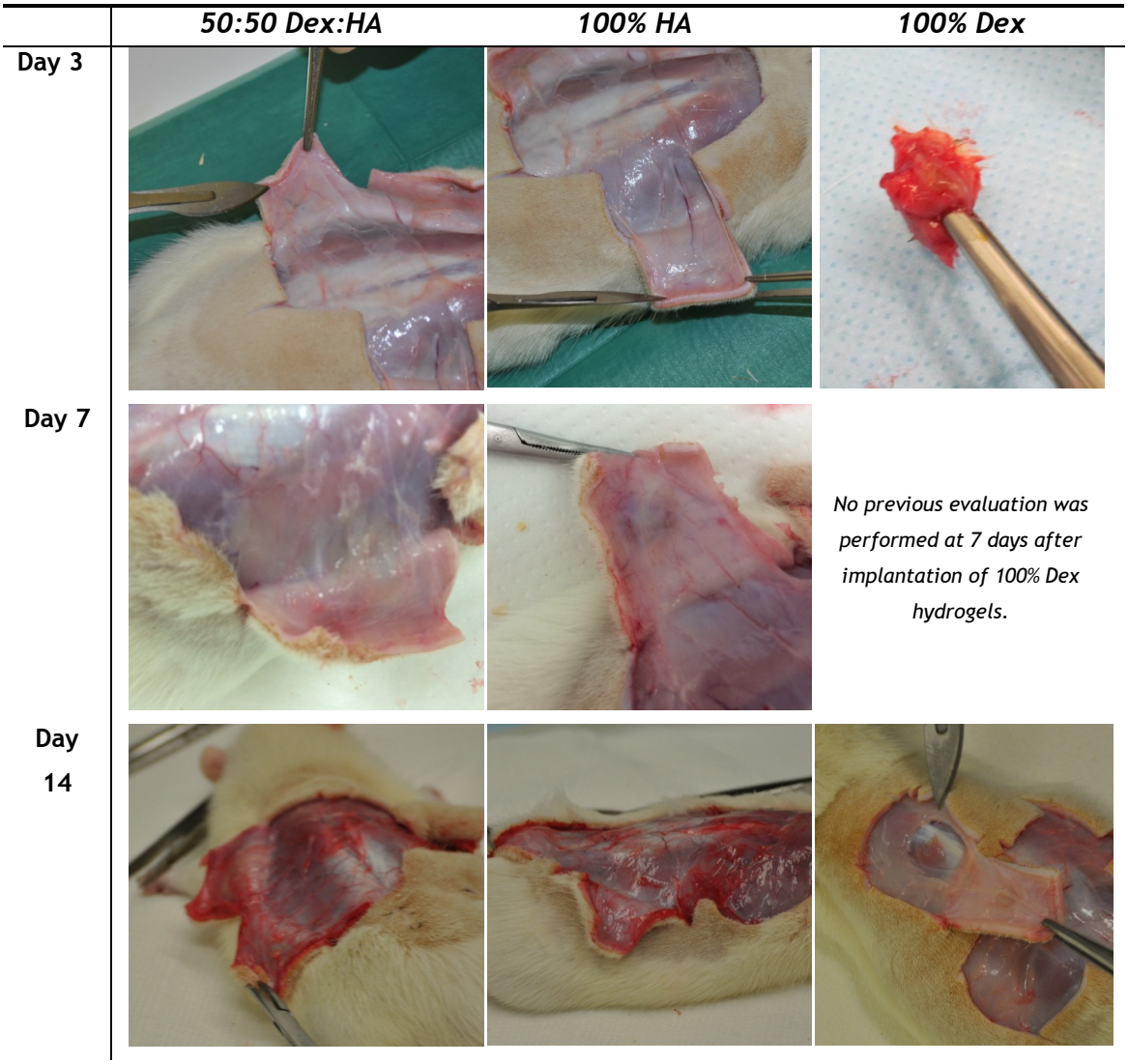

Figure 4.20. Macroscopic analysis of the subcutaneously implantation of Dex and HA hydrogels in the lumbar region of the rats.

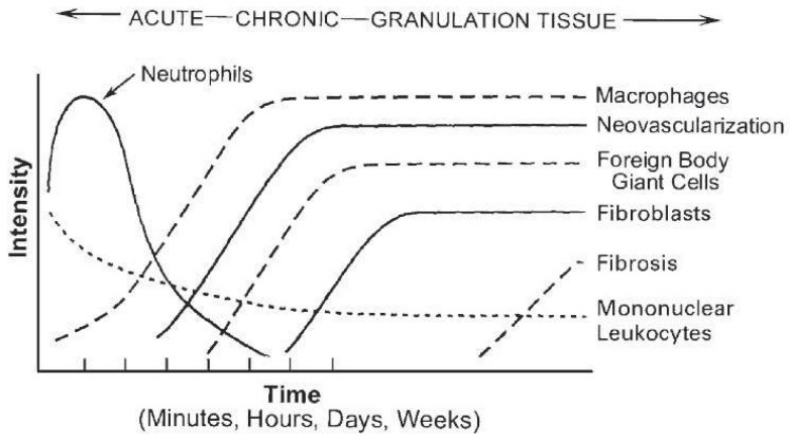

Figure 4.21. Relative intensity of different cell levels during inflammatory response [57].

In histological analysis, quantitative scoring is given for each histological characteristic evaluated, such as capsule formation, inflammation and presence of giant cells, comparing the tissue in analysis with the negative control sample. The quantitative score is based on Tables 4.4 and 4.5 and this evaluation system can be converted to an implant evaluation system as described in Table 4.6. Control sample corresponds to the inflammatory response of the surgery. Under the conditions observed and the obtained score, the test sample can be considered non-irritant (0.0 up to 2.9), slight irritant (3.0 up to 8.9), moderate irritant (9.0 up to 15.0) or severe irritant (over 15.0) [59].

Table 4.4. Histological evaluation system based on cell type/response. phf stands for per high powered (400x) field [59].

Cell type/response	Score				
	0	1	2	3	4
Polymorphonuclear cells	0	Rare, 1-5/phf	5-10/phf	Heavy infiltrate	Packed
Lymphocytes	0	Rare, 1-5/phf	5-10/phf	Heavy infiltrate	Packed
Plasma cells	0	Rare, 1-5/phf	5-10/phf	Heavy infiltrate	Packed
Macrophages	0	Rare, 1-5/phf	5-10/phf	Heavy infiltrate	Packed
Giant cells	0	Rare, 1-2/phf	3-5/phf	Heavy infiltrate	Sheets
Necrosis	0	Minimal	Mild	Moderate	Severe

Table 4.5. Histological evaluation based on tissue response [59].

Tissue response	Score				
	0	**1**	**2**	**3**	**4**
Neovascularisation	0	Minimal capillary proliferation, focal, 1-3 buds	Groups of 4-7 capillaries with supporting fibroblastic structures	Broad band of capillaries with supporting structures	Extensive band of capillaries with supporting fibroblastic structures
Fibrosis	0	Narrow band	Moderately thick band	Thick band	Extensive band
Fatty infiltrate	0	Minimal amount of fat associated with fibrosis	Several layers of fat and fibrosis	Elongated and broad accumulation of fat cells about the implant site	Extensive fat completely surrounding the implant

Table 4.6. Semi-quantitative evaluation system. [a] Used to determine irritant ranking. A negative difference is recorded as zero [59].

Test sample:	Implantation interval:					
	Test sample			Control sample		
Inflammation Polymorphonuclear cells						
Lymphocytes						
Plasma cells						
Macrophages						
Giant cells						
Necrosis						
SUB-TOTAL (X2)						
Neovascularisation						
Fibrosis						
Fatty infiltrate						
SUB-TOTAL						
TOTAL						
GROUP TOTAL						
AVERAGE [a]	TEST (-) CONTROL =					
Traumatic necrosis						
Foreign debris						
No. sites examined						

Evaluation was performed using the Sham group (control with no implant but where the suture was performed) with the quantitative score of 15.33, 15.33 and 14.11 for 3, 7 and 14 days of implantation, respectively. After performing this evaluation, results (Table 4.7)

indicate that 50:50 Dex:HA hydrogels were slight irritant during the 14 days period. On the other hand, 100% HA hydrogels were non-irritant 3 days after implantation and slight irritant after that time. In contrast, 100% Dex hydrogels were slight irritant 3 days after implantation and non-irritant after 14 days. Since 100% Dex hydrogels have a high degradation rate, after 14 days the hydrogel was already degraded, decreasing the inflammatory response and evaluating the hydrogel as non-irritant. However, due to the lower degradation rate 100% HA and 50:50 Dex:HA hydrogels were still present, causing an inflammatory response. As long as the hydrogel is not degraded, an inflammatory reaction will occur.

Table 4.7. Quantitative scoring of histocompatibility for 50:50 Dex:HA, 100% HA and 100% Dex hydrogels for 3, 7 and 14 days after implantation.

	3 days	7 days	14 days
50:50 Dex:HA hydrogel	6.3 (slight irritant)	7.2 (slight irritant)	8.9 (slight irritant)
100% HA Hydrogel	2.0 (non-irritant)	8.0 (slight irritant)	6.4 (slight irritant)
100% Dex Hydrogel	4.1 (slight irritant)	-	2.1 (non-irritant)

Three days after the implantation of 50:50 Dex:HA hydrogels (Figure 4.22) it is possible to observe high levels of neutrophils, lymphocytes and active macrophages. Mild necrosis is also present. After 7 days of implantation (Figure 4.23), the number of neutrophils decreased, as well as necrosis. Giant cells were present associated with foreign body reaction caused, for instance by hair and probably increasing the inflammatory levels. In addition, fibrosis slightly increased. Mild oedema was also present. At 14 days after implantation (Figure 4.24), the number of active macrophages decreased and the number of giant cells increased. The latter were strongly associated with foreign bodies probably increasing the final score. At this point, neovascularisation and fibrosis also increased.

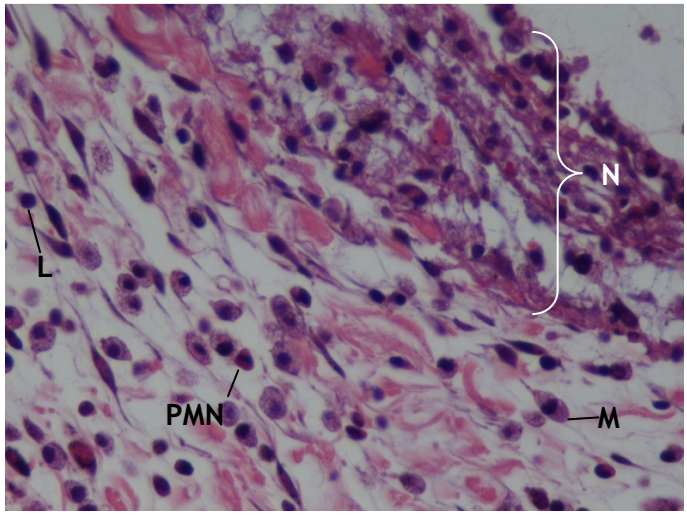

Figure 4.22. Histological analysis of the subcutaneously implantation of 50:50 Dex:HA hydrogels in the lumbar region of the rats after 3 days where is possible to observe necrosis (N), neutrophils (PMN), lymphocytes (L) and macrophages (M) (HE, amplification: 200x).

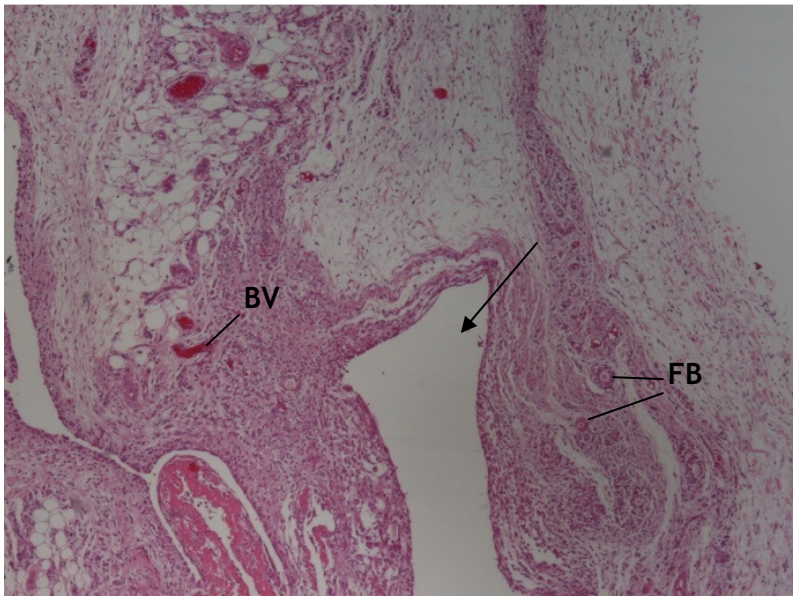

Figure 4.23. Histological analysis of the subcutaneously implantation of 50:50 Dex:HA hydrogels in the lumbar region of the rats after 7 days where is possible to observe the implantation site (arrow), blood vessels (BV) and foreign bodies (FB) (HE, amplification: 40x).

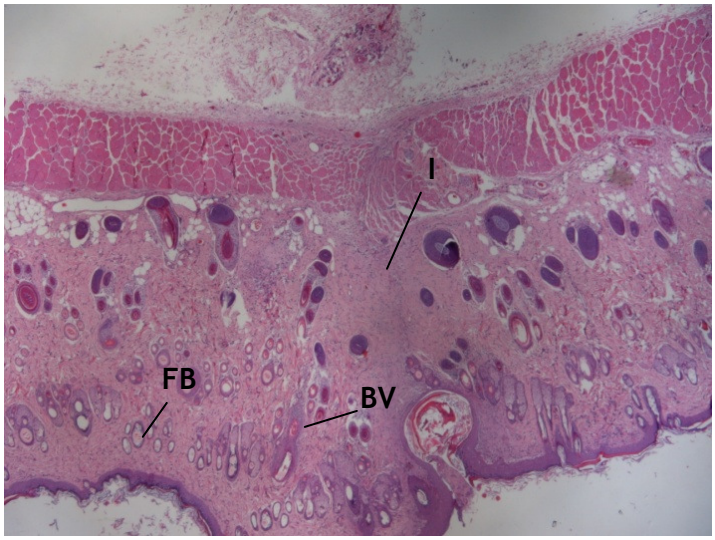

Figure 4.24. Histological analysis of the subcutaneously implantation of 50:50 Dex:HA hydrogels in the lumbar region of the rats after 14 days where is possible to observe the incision site (I), blood vessels (BV) and foreign bodies (FB) (HE, amplification: 20x).

Regarding 100% HA hydrogels, after 3 days of implantation high levels of neutrophils and macrophages were present, suggestive of a subacute inflammatory response. In addition, mild neovascularisation was observed and few lymphocytes and plasma cells were found, which accounts for the low quantitative score. After 7 days of implantation (Figure 4.25), giant cells were found as well as an increased number of lymphocytes. More neovascularisation and mild

fibrosis were also observed and a thick fibrotic capsule surrounding the implantation site was present. At 14 days after implantation (Figures 4.26 and 4.27) it was still possible to observe few traces of hydrogel. At this point, no necrosis nor neutrophils were found. Lymphocytes levels were increased and minimal fibrosis was observed. In contrast with other hydrogels, fatty infiltrate was found.

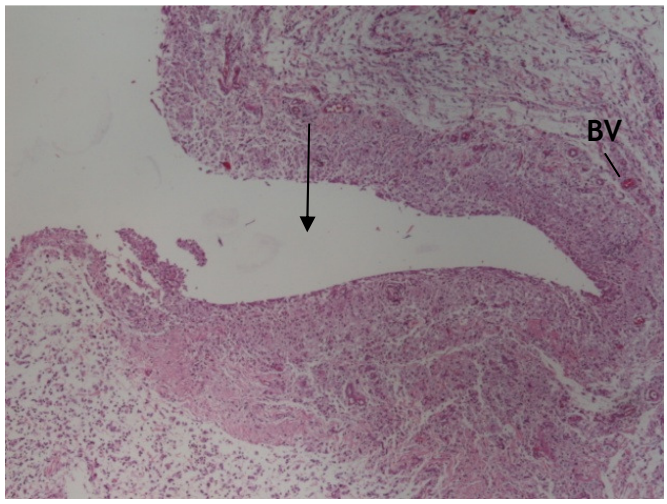

Figure 4.25. Histological analysis of the subcutaneously implantation of 100% HA hydrogels in the lumbar region of the rats after 7 days where is possible to observe the implantation site (arrow) and blood vessels (BV) (HE, amplification: 40x).

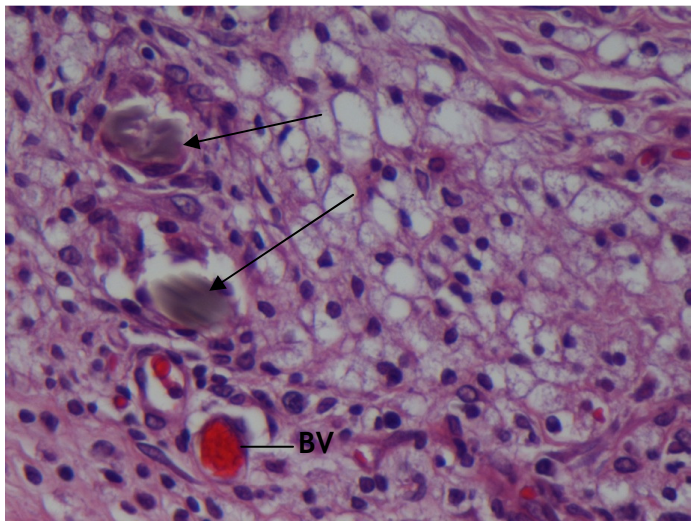

Figure 4.26. Histological analysis of the subcutaneously implantation of 100% HA hydrogels in the lumbar region of the rats after 14 days where is possible to observe a few tracesof the hydrogel (arrows) and blood vessels (BV) (HE, amplification: 400x).

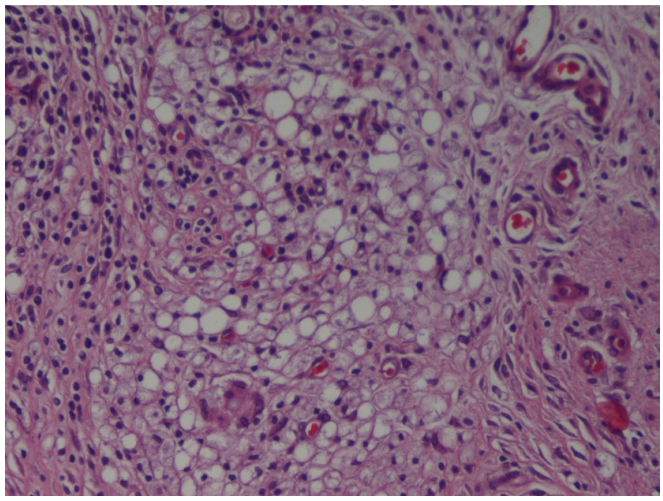

Figure 4.27. Histological analysis of the subcutaneously implantation of 100% HA hydrogels in the lumbar region of the rats after 14 days where is possible to observe fatty infiltrate (HE, amplification: 200x).

100% Dex hydrogels caused fibrinoid necrosis after 3 days of implantation (Figure 4.28). High levels of neutrophils, lymphocytes, macrophages and neovascularisation were present in this inflammatory reaction which indicates the transition between acute to chronic inflammations. At 14 days of implantation (Figure 4.29) higher levels of fibrosis and neovascularisation were present but there was a decrease in neutrophils levels and necrosis which is compatible with tissue formation.

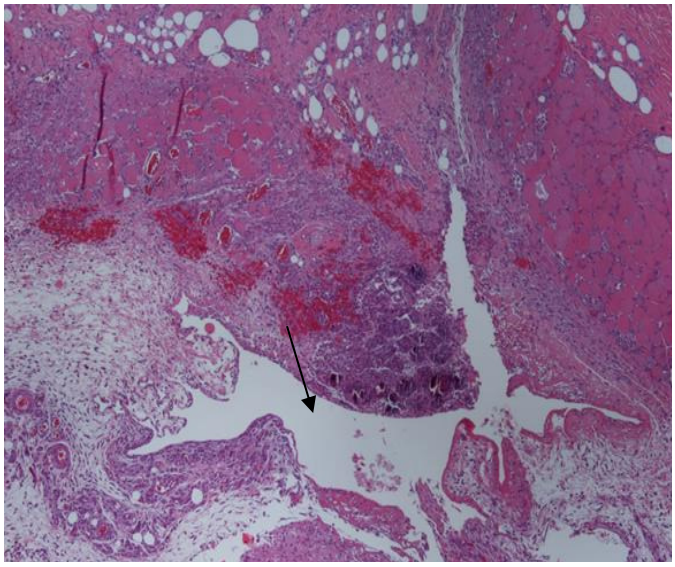

Figure 4.28. Histological analysis of the subcutaneously implantation of 100% Dex hydrogels in the lumbar region of the rats after 3 days. It is possible to observe the implantation site (arrow) (HE, amplification: 40x).

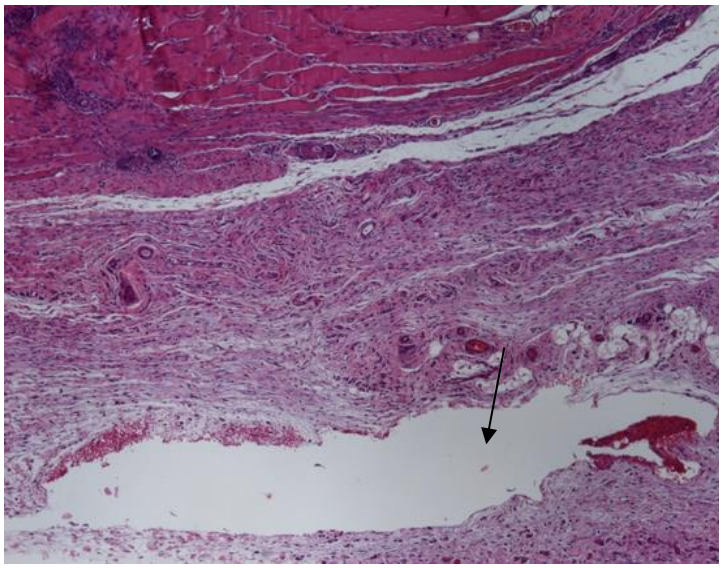

Figure 4.29. Histological analysis of the subcutaneously implantation of 100% Dex hydrogels in the lumbar region of the rats after 14 days. It is possible to observe the implantation site (arrow) (HE, amplification: 40x).

Although the higher quantitative scoring of 50:50 Dex:HA hydrogels compared to the ones obtained with 100% HA and 100% Dex hydrogels, no fibrous capsule or fatty infiltrate was present in the inflammatory reaction which can suggest that mixed hydrogels have an appropriate histocompatibility.

Chapter 5

Conclusions

Due to their different properties, several types of HA were tested with Dex using different proportions. The production of the hydrogels revealed that high MW HA and CL-HA have low solubility, resulting in highly viscous hydrogels. Consequently, a lower gelation time was observed with an increase in the percentage of HA. In addition high MW HA and CL-HA hydrogels polymerized in the eppendorf without the crosslinking agent.

The obtained DO of oxidized Dex was lower than the theoretical value, in agreement with the literature. Due to the low solubility of CL-HA, aldehyde groups were very difficult to quantify so it was not possible to measure the experimental DO for oxidized CL-HA.

Degradation assays revealed that 100% Dex hydrogels and low MW HA hydrogels have higher degradation rates due to their high solubility and high water affinity. On the other hand, hydrogels with higher MW HA and higher HA contents revealed a low degradation rate, suggesting that the weight loss increases with the Dex contents. Several factors may influence the degradation behaviour besides the MW such as hydrophilicity of the materials, porosity and osmotic forces. In some hydrogels a swelling phase was observed which can be important for cell survival. Mixed hydrogels bear a steady rate of mass loss in contrast with 100% HA hydrogels which displayed an initial low degradation rate followed by a rather fast degradation. Due to its lower degradation rate, the 50:50 Dex:CL-HA was chosen for the following tests.

Resazurin assays were used to account for cell viability using MG-63 cells during 7 days and indicated that *in vitro* MG-63 cells in 50:50 Dex:HA hydrogels had very low viability in comparison with MG-63 cells in 100% HA hydrogels and with the cellular control. This may be due to the lattice of 50:50 Dex:HA hydrogels that may enclosure non-linked ADH or due to the exposure of free aldehyde groups. Another resazurin assay performed 5h after the production

of 100% Dex hydrogels showed higher values for MG-63 cells in the hydrogels than in the cellular control which, due to the processes involved, suggest a higher cellular adhesion in the hydrogels than in plastic. A MTT assay was also performed and revealed that Dex and HA interfere with MTT, presenting false positive results.

Histocompatibility assays were performed by implanting subcutaneously 50:50 Dex:HA and 100% HA hydrogels in the lumbar region of rats. Macroscopic observation of the implantation site revealed no necrosis or fibrosis during the 14 days period. Histological analysis indicated that 50:50 Dex:HA hydrogels were slight irritant during the 14 days. On the other hand, 100% HA hydrogels were non-irritant 3 days after implantation and slight irritant after that time. In contrast, 100% Dex hydrogels were slight irritant 3 days after implantation and non-irritant after 14 days. This can be explained by differences in the degradation rate.

These tests indicate that a hydrogel produced with Dex and HA has the potential to maintain MSCs but further research is necessary to better characterize the hydrogels and its biological functions. The DO of HA should be determined using low MH HA due to its high solubility. Optimization of the production of the hydrogels should be performed to reduce free aldehyde groups, changing either the DO and/or the ADH concentration. Consequently, an optimization of the characteristics of the hydrogel should also occur by varying several factors including the polymer concentration, the DO and the proportion of Dex and HA. Viability tests should be performed using techniques that do not cause false positive results and more assays should be performed to validate the obtained results. Due to their different biological characteristics, different types of HA should be used in these assays. The negative charge of HA provides high water binding capability and water absorption capacity, creating a large porous matrix space and promoting cellular migration so a cryo-SEM should be performed to study the topography and porosity of the hydrogels.

While it is possible that osteosarcoma cells represent a suitable model for studying osteoblastic differentiation on biomaterials, it is not yet clear that these cells mimic the behaviour of MSCs during the initial phases of cell attachment to a biomaterial so further testing should be performed using fresh and cryopreserved MSCs for comparison. The duration of the undifferentiated state in mixed hydrogels should be tested for long test periods until the MSCs in the control differentiate. This characterization can be done using cytogenetic analysis, analysis of gene expression by RT-PCR and microbiological assays to test for osteogenic or chondrogenic differentiation in different time points. Quantification of ALP activity can be used as a marker for osteoblast differentiation.

Support Material

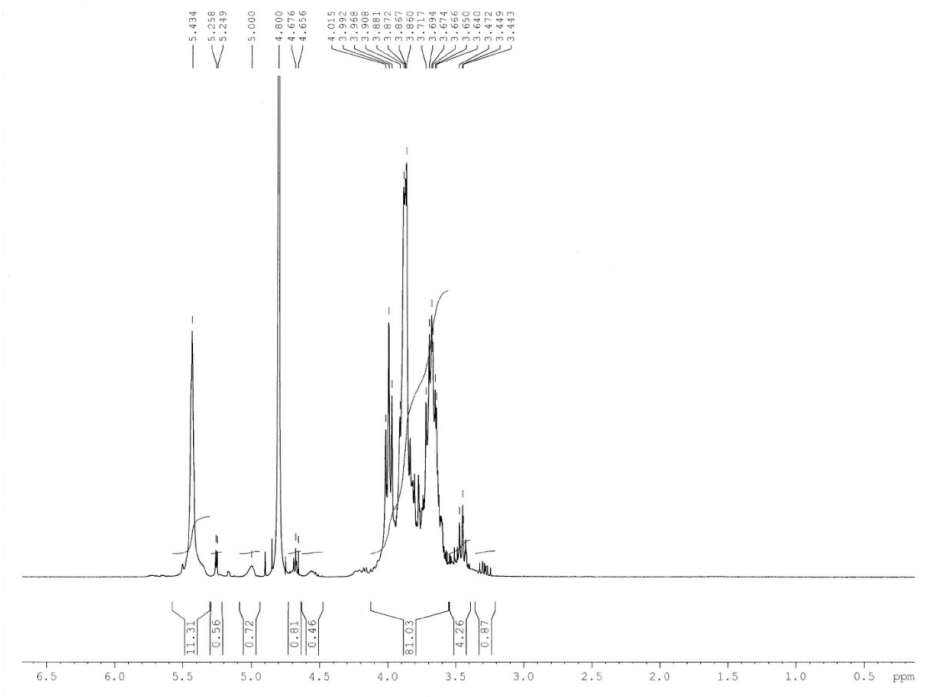

Figure S1. ^{1}H NMR spectrum of Dex.

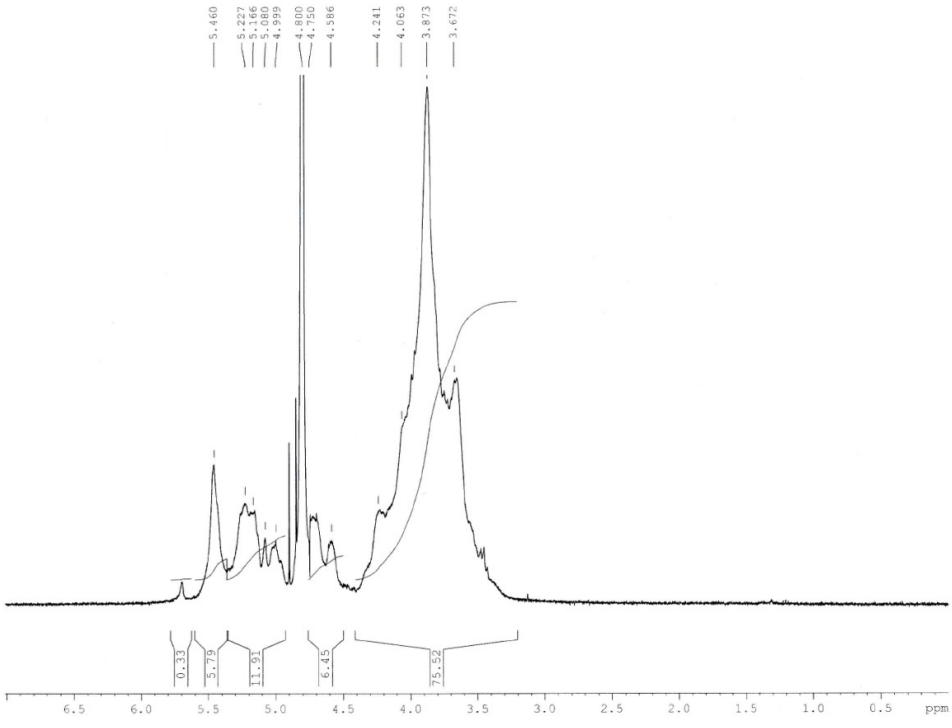

Figure S2. ^{1}H NMR spectrum of oxidized Dex.

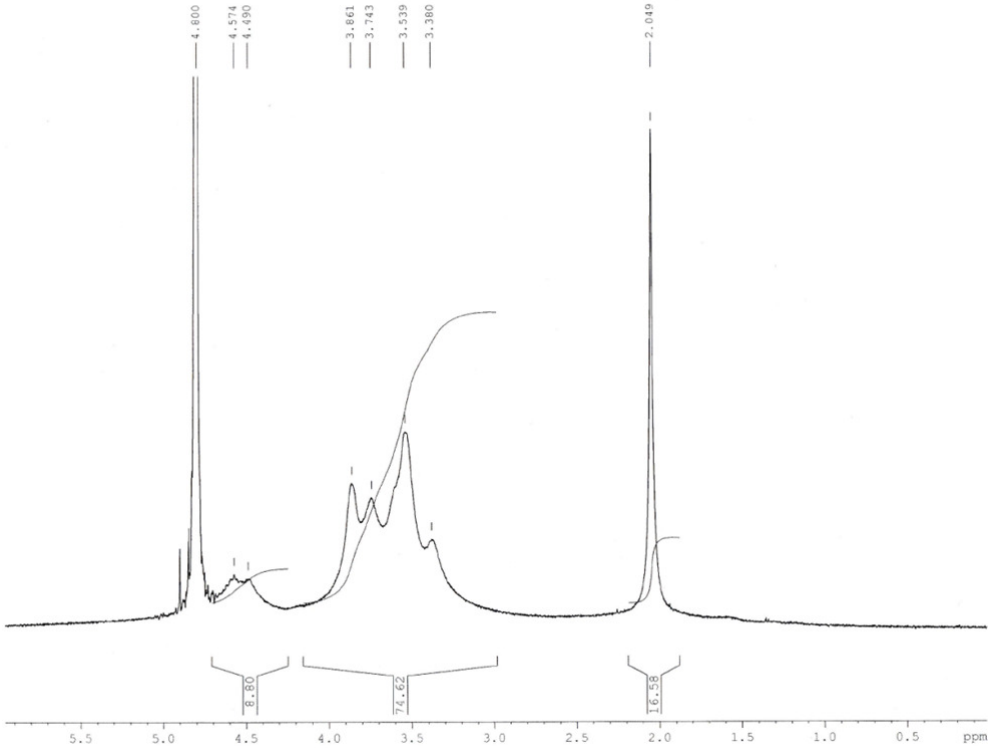

Figure S3. ^{1}H NMR spectrum of CL-HA.

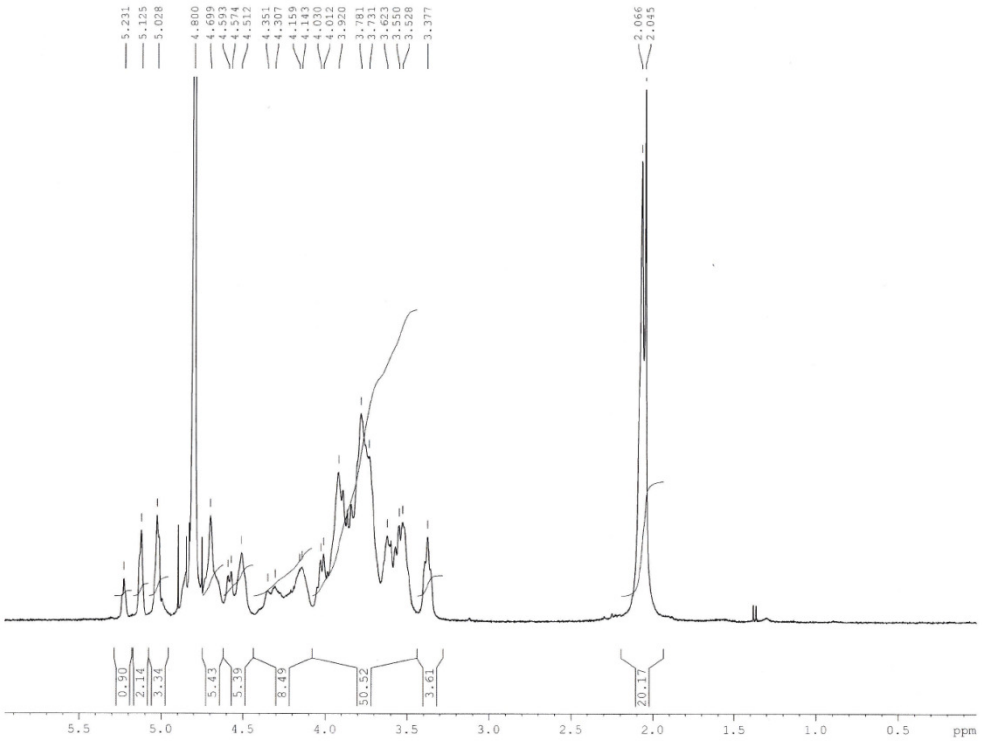

Figure S4. ^{1}H NMR spectrum of oxidized CL-HA.

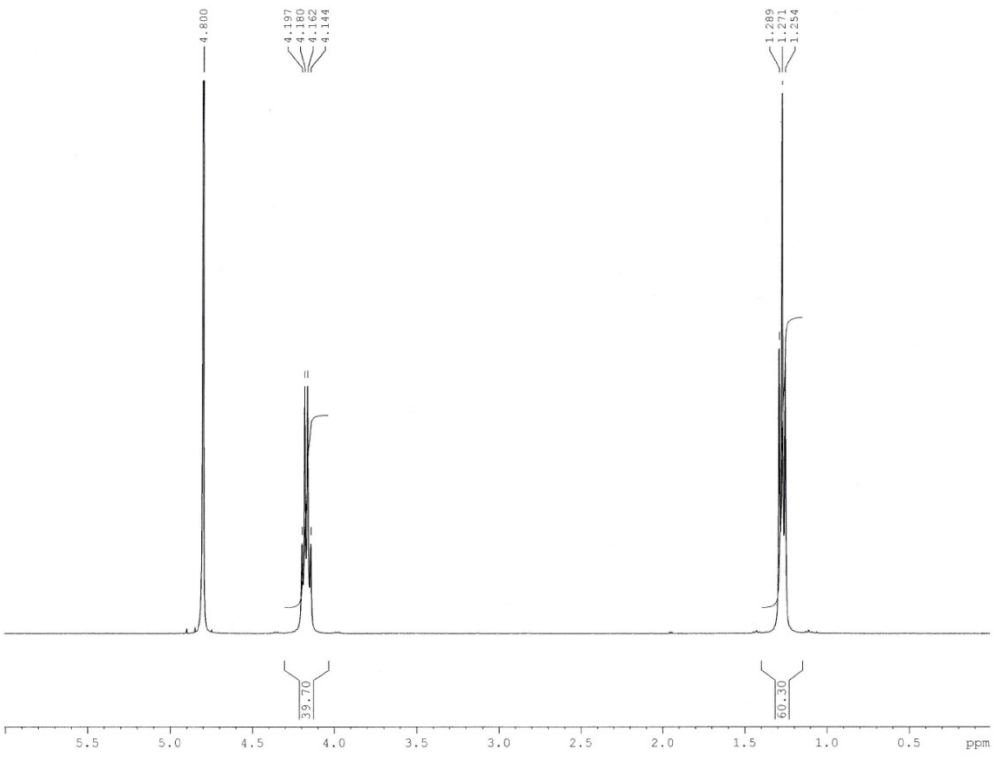

Figure S5. ^{1}H NMR spectrum of ETC.

References

[1] Chen YC, Su WY, Yang SH, Gefen A, Lin FH. In situ forming hydrogels composed of oxidized high molecular weight hyaluronic acid and gelatin for nucleus pulposus regeneration. Acta Biomaterialia 2013, 9:5181-5193.

[2] Tsai CC, Su PF, Huang YF, Yew TL, Hung SC. Oct4 and Nanog directly regulate Dnmt1 to maintain self-renewal and undifferentiated state in mesenchymal stem cells. Molecular Cell 2012, 47:169-182.

[3] Iacono ML, Anzalone R, Corrao S, Giuffrè M, Stefano AD, Giannuzzi P *et al*. Perinatal and Wharton's jelly-derived mesenchymal stem cells in cartilage regenerative medicine and tissue engineering strategies. The Open Tissue Engineering and Regenerative Medicine Journal 2011, 4:72-81.

[4] Segura T, Anderson BC, Chung PH, Webber RE, Shull KR, Shea LD. Crosslinked hyaluronic acid hydrogels: a strategy to functionalize and pattern. Biomaterials 2005, 26:359-371.

[5] Burdick JA, Chung C, Jia X, Randolph MA, Langer R. Controlled degradation and mechanical behavior of photopolymerized hyaluronic acid networks. Biomacromolecules 2005, 6:386-391.

[6] Gerecht S, Burdick JA, Ferreira LS, Townsend SA, Langer R. Hyaluronic acid hydrogel for controlled self-renewal and differentiation of human embryonic stem cells. PNAS 2007, 104(27):11298-11303.

[7] Ishige I, Nagamura-Inoue T, Honda MJ, Harnprasopwat R, Kido M, Sugimoto M, Nakauchi H, Tojo A. Comparison of mesenchymal stem cells derived from arterial, venous, and Wharton's jelly explants of human umbilical cord. International Journal of Hematology 2009, 90:261-269.

[8] Laurance Johnson. Stem Cells. Available at http://www.sci-therapies.info/Stem-Cells.htm. Access on 15/12/2013.

[9] Sethe S, Scutt An, Stolzing A. Aging of mesenchymal stem cells. Ageing Research Reviews 2006, 5:91-116.

[10] Astachov L, Vago R, Aviv M, Nevo Z. Hyaluronan and mesenchymal stem cells: from germ layer to cartilage and bone. Frontiers in Bioscience 2011, 16:261-276.

[11] College of Engineering, University of Wisconsin-Madison. Umbilical Vein Catheterization Model. Available at http://homepages.cae.wisc.edu/~bme300/umbilical_f07/. Access on 20/11/2013.

[12] Family Research Council. Plentiful Stem Cells from Umbilical Cord. Available at http://www.frcblog.com/2009/12/plentiful-stem-cells-from-umbilical-cord/. Access on 20/11/2013.

[13] Nanaev AK, Kohnen G, Milovanov AP, Domogatsky SP, Kaufmann P. Stromal differentiation and architecture of the human umbilical cord. Placenta 1997, 18:53–64.

[14] Baksh D, Yao R, Tuan RS. Comparison of proliferative and multilineage differentiation potential of human mesenchymal stem cells derived from umbilical cord and bone marrow. Stem Cells 2007, 25:1384–92.

[15] Mitchell KE, Weiss ML, Mitchell BM, Martin P, Davis D, Morales L, *et al*. Matrix cells from Wharton's jelly form neurons and glia. Stem Cells 2003, 21:50–60.

[16] Wang L, Sheshareddy K, Weiss ML, Detamore MS. Effect of initial seeding density on human umbilical cord mesenchymal stromal cells for fibrocartilage tissue engineering. Tissue Eng Part A 2009, 15:1009-17.

[17] Zhang D, Kilian KA. The effect of mesenchymal stem cell shape on the maintenance of multipotency. Biomaterials 2013, 34:3962-3969.

[18] Toyoda M, Takahashi H, Umezawa A. Ways for a mesenchymal stem cell to live on its own: maintaining an undifferentiated state ex vivo. International Journal of Hematology 2007, 86:1-4.

[19] Basciano L, Nemos C, Foliguet B, Isla N, Carvallo M, Tran N, Dalloul A. Long term culture of mesenchymal stem cells in hypoxia promotes a genetic program maintaining their undifferentiated and multipotent status. BMC Cell Biology 2011, 12:12.

[20] Grayson WL, Zhao F, Izadpanah R, Bunnell B, Ma T. Effects of hypoxia on human mesenchymal stem cell expansion and plasticity in 3D constructs. J Cell Physiol 2006, 207:331-339.

[21] Vohra S, Hennessy KM, Sawyer A, Zhuo Y, Bellis SL. Comparison of mesenchymal stem cell and osteosarcoma cell adhesion to hydroxyapatite. J Mater Sci: Mater Med 2008, 19:3567-3574.

[22] Billiau A, Cassiman JJ, Willems D, Verhelst M, Heremans H. In vitro cultivation of human tumor tissues. Oncology 1975, 31:257-272.

[23] Lajeunesse D, Frondoza C, Schoffield B, Sacktor B. Osteocalcin secretion by the human osteosarcoma cell line MG63. J Bone Miner Res 1990, 5:915-922.

[24] Carmeliet G, Nys G, Boullion R. Microgravity reduces the differentiation of human osteoblastic MG-63 cells. Journal of Bone and Mineral Research 1997, 12 (5):786-794.

[25] Pautke C, Schieker M, Tischer T, Kolk A, Neth P *et al*. Characterization of osteosarcoma cell lines MG-63, Saos-2 and U-2 OS in comparison to human osteoblasts. Anticancer Research 2004, 24:3743-3748.

[26] Akiyama Y, Mikami Y, Watanabe E, Watanabe N, Toriumi T *et al*. The P75 neurotrophin receptor regulates proliferation of the human MG63 osteoblast cell line. Differentiation 2014.

[27] Lou N, Wang Y, Sun D, Zhao J, Wang Y, Gao Z. Isolation of stem-like cells from human MG-63 osteosarcoma cells using limiting dilution in combination with vincristine selection. Indian Journal of Biochemistry & Biophysics 2010, 47:340-347.

[28] Molinos M, Carvalho V, Silva DM, Gama FM. Development of a hybrid dextrin hydrogel encapsulating dextrin nanogel as protein delivery system. Biomacromolecules 2012, 13:517-527.

[29] Aurand ER, Wagner JL, Shandas R, Bjugstad KB. Hydrogel formulation determines cell fate of fetal and adult neural progenitor cells. Stem Cell Research 2014, 12:11-23.

[30] Wei YT, Cui FZ, Tian WM. Fabrication and characterization of hyaluronic-acid-based antigen sensitive degradable hydrogel. Front. Master. Sci. China 2009, 3(4):353-358.

[31] Su WY, Chen YC, Lin FH. Injectable oxidized hyaluronic acid/adipic acid dihydrazide hydrogel for nucleus pulposus regeneration. Acta Biomaterialia 2010, 6:3044-3055.

[32] Prestwich GD, Marecak DM, Marecek JF, Vercruysse KP, Ziebell MR. Controlled chemical modification of hyaluronic acid: synthesis, applications, and biodegradation of hydrazide derivatives. Journal of Controlled Release 1998, 53:93-103.

[33] Xu X, Jha AK, Harrington DA, Farach-Carson MC, Jia X. Hyaluronic acid-based hydrogels: from a natural polyssacharide to complex networks. Soft Matter. 2012, 8(12):3280-3294.

[34] Noble P. Hyaluronan and its catabolic products in tissue injury and repair. Matrix Biology 2002, 21:25-29.

[35] Assman V, Jenkinson D, Marshall J, Hart I. The intracellular hyaluronan receptor RHAMM/IHABP interacts with microtubules and actin filaments. J. Cell. Sci. 1999 112(22):3943-3954.

[36] Carvalho J, Gonçalves C, Gil AM, Gama FM. Production and characterization of a new dextrin based hydrogel. European Polymer Journal 2007, 43:3050-3059.

[37] Teixeira-Dias B, Valle LJ, Estrany F, Mano JF, Reis RL, Alemán C. Dextrin- and conducting-polymer-containing biocomposites: properties and behavior as cellular matrix. Macromolecular Materials and Engineering 2012, 297, 359-368.

[38] Moreira SM, Andrade FK, Domingues L, Gama FM. Development of a strategy to functionalize a dextrin-based hydrogel for animal cell cultures using a starch-binding module fused to RGD sequence. BMC Biotechnology 2008, 8:78.

[39] Hardwicke J, Moseley R, Stephens P, Hardling K, Duncan R, Thomas DW. Bioresponsive dextrin-rhEGF conjugates: in vitro evaluation in models relevant to its proposed use as a treatment for chronic wounds. Molecular Pharmaceutics 2010, 7(3):699-707.

[40] Ferreira LAR, Lamghari M, Barbosa MA, Gil MH, Cabrita AMS, Dordick JS. Biocompatibility of chemoenzymatically derived dextran-acrylate hydrogels. Journal of Biomedical Materials Research Part A 2004, 68(3):584-596

[41] Bouhadir KH, Hausman DS, Mooney DJ. Synthesis of cross-linked poly(aldehyde guluronate) hydrogels. Polymer 1999, 40:3575-3584.

[42] Stern R, Asari AA, Sugahara KN. Hyaluronan fragments: an information-rich system. European Journal of Cell Biology 2006, 85:699-715.

[43] Novozymes. Hyasis ® Link – Hyaluronic acid crosslinking technology. Available at http://www.biopharma.novozymes.com/en/hyaluronic-acid/Crosslinking-technology/Pages/default.aspx. Access on 4/5/2014

[44] Kim J, Park Y, Tae G, Lee KB, Hwang CM *et al*. Characterization of low-molecular-weight hyaluronic acid-based hydrogel and differential stem cell responses in the hydrogel microenvironments. Journal of Biomateral Materials Research Part A 2008, 967-975.

[45] Maia J, Ferreira L, Carvalho R, Ramos MA, Gil MH. Synthesis and characterization of new injectable and degradable dextran-based hydrogels. Polymer 2010, 46:9604-9614.

[46] Bodnár M, Daróczi L, Batta G, Bakó J, Hartmann JF, Borbély J. Preparation and characterization of cross-linked hyaluronan nanoparticles. Colloid Polym Sci 2009, 287:991-1000.

[47] Maia J, Carvalho RA, Coelho JFJ, Simões PN, Gil MH. Insight on the periodate oxidation of dextran and its structural vicissitudes. Polymer 2011, 52:258-265.

[48] Carvalho JM, Gama FM. Hydrogels of enzymatically modified dextrin. In "Proceedings of the 2nd Mercosur Congress on Chemical Engineering – ENPROMER and 4th Mercosur Congress on Process Systems Engineering" 2005.

[49] Linh NTB, Min YK, Lee BT. Fabrication and in vitro evaluations with osteoblast-like MG-63 cells of porous hyaluronic acid-gelatin blend scaffold for bone tissue engineering applications. J Mater Sci 2013, 48:4233-4242.

[50] Hoffman AS. Hydrogels for biomedical applications. Advanced Drug Delivery Reviews 2002, 54:3-12.

[51] Chen C, Chen K, Yang ST. Effects of three-dimensional culturing on osteosarcoma cells grown in a fibrous matrix: analyses of cell morphology, cell cycle, and apoptosis. Biotechnology Progress 2003, 19(5):1574-1582.

[52] Huang-Lee LL, Cheung DT, Nimni ME. Biochemical changes and cytotoxicity associated with the degradation of polymeric glutaraldehyde derived crosslinks. Journal of Biomedical Materials Research 1990, 24(9):1185-1201.

[53] Mcpherson IM, Sawamura S, Armstrong R. An Examination of the Biologic Response to Injectable, Glutaraldehyde Cross-Linked Collagen Implants. Journal of Biomedical Materials Research 1986, 20(1):93-107.

[54] Furst W, Banerjee A. Release of glutaraldehyde from an albumin-glutaraldehyde tissue adhesive causes significant in vitro and in vivo toxicity. Annals of Thoracic Surgery 2005, 579 79(5):1522-1529.

[55] Chang W, Lim S, Song H, Lee S, Song BW *et al*. In vitro expansion of mesenchymal stem cells using 3-D matrix derived from cardiac fibroblast. Tissue Engineering and Regenerative Medicine 2007, 4(3):370-375.

[56] Anderson JM, Rodriguez A, Chang DT. Foreign body reaction to biomaterials. Seminars in Immunology 2008, 20:86-100.

[57] Davies JE. Immediate loading: The role of the implant surface on biological stabilization. Journal of Implant and Reconstructive Dentistry 2010, 2(1):10-17.

[58] Gulrez SKH, Al-Assaf S, Phillips GO. Hydrogels: methods of preparation, characterisation and applications. Progress in Molecular and Environmental Bioengineering – From Analysis and Modelling to Technology Applications 2011. Prof. Angelo Carpi (Ed.), InTech.

[59] ISO 10993-6, Biological evaluation of medical devices – Part 6: Tests for local effects after implantation.